Pathological extracellular matrix suppresses microRNA-29 at the level of microRNA processing in Idiopathic Pulmonary Fibrosis

A Dissertation
SUBMITTED TO THE FACULTY OF
UNIVERSITY OF MINNESOTA
BY

Jeremy Alexander Herrera

IN PARTIAL FULFILLMENT OF THE REQUIREMENTS
FOR THE DEGREE OF
DOCTOR OF PHILOSOPHY

Peter Bitterman, MD

June 2015

Acknowledgements

Earning a PhD in Cancer Biology is not a simple walk through the park. It has been a long journey, and as cliché as it may be, perseverance is key. Several people have been critical during this journey, and I could not have been successful without them. My work could not have been accomplished without my advisor, Pete Bitterman. The most admiring thing about Pete is his ability to interpret data. This project yielded unexpected experimental outcomes, but Pete always had a reasonable explanation. He is respectful, supportive, and encouraging. It has been a pleasure working under his advisement, and I cannot thank him enough. The Bitterman Lab is a pleasant place to work. I enjoy coming in to work every day because it is a family that cares about your wellbeing and academic success. It feels like home, and how many people can say that about their work place?

I would also like to acknowledge Vitaly Polunovsky for his passion. Without his passion, we would not have published the eIF4E story. He was the driving force, and it was definitely an experience from start to finish. I would also like to equally acknowledge Craig Henke. Craig was down the hall and he always gave great feedback when discussing data. Craig wants me to succeed, and I am successful because of his contribution in training me in fibroblast biology.

Another critical component of my PhD journey was my training in histological stains. Colleen Forster trained me to be the histologist I am today. I have learned a variety of techniques, and constantly work to perfect each stain with the hopes to achieving the highest of quality. Without her training, I would not have been so successful in all my co-authored work.

I would lastly like to acknowledge Mark Peterson. Mark has always been the ‘to go to guy’ to discuss data or planned experiments. Half the time we discuss non-science related topics (such as Game of Thrones or current events) but the other half we are engaged in scientific discussions. Most of the time when I have an idea, I run to Mark to help me decide if I am crazy, or perhaps I am on to something. He looks at things in an unbiased way and we work well together. My PhD journey will not have been completed without the advisement of Peter Bitterman, Vitaly Polunovsky, Craig Henke, Colleen Forster, and Mark Peterson. Thanks so much everyone!

Dedication

This thesis is dedicated to those who suffer from Idiopathic Pulmonary Fibrosis and their families. We are invested in unraveling the mechanism of thesis so that we may one day target points of vulnerability in its genesis.

I also dedicate this thesis to my family who has always been supportive of me. It has definitely been a long academic journey, and now I have a PhD degree to show for it. I was raised to make the right decisions, and I was raised to do whatever it was I dreamed to be. I will continue to make you guys proud as I progress into the next step of my career.

Table of Contents

List of Figures

Chapter A.1: An introduction to Idiopathic Pulmonary Fibrosis

Idiopathic Pulmonary Fibrosis (IPF) is a lethal disease that is defined by the accumulation of fibroblasts and excessive deposition of extracellular matrix (ECM) between the alveolar surfaces of the lung. The pathological feature in IPF is the hallmark lesion called the fibroblastic focus. Fibroblastic foci are sites where proliferative fibroblast cells accumulate (between alveolar surfaces), deposit excess ECM, and contract alveolar walls compromising oxygen exchange which results in asphyxiation of patients. Currently, there are two pharmacological approved drugs to treat the progression of disease: Pirfenidone and Ninetdanib [Tzouvelekis 2015], although the most beneficial treatment is double lung transplantation [Schaffer 2015]. Clinical features of IPF include that it predominantly affects men, rarely presents in patients under the age of 50, and has a median survival of 3 years after diagnosis; IPF affects 2 million people worldwide with a prevalence of 50 per 100,000, and kills about 40,000 Americans a year (comparable to breast cancer related deaths a year) [Wolters 2013]. Although there are cases of hereditary IPF (20% of cases), IPF is not a genetic disease. IPF has been linked with genetic alterations of mucin 5B (MUC5B), telomerase (TERT/TERC), and surfactant protein C and A2 (SPC and SPA, respectively) although there are no data to support that these directly lead to lung fibrosis [Wolters 2013]. IPF is a progressive lethal disease and identifying points of vulnerability in its pathogenesis is warranted.

Chapter A.2. The cellular components of Idiopathic Pulmonary Fibrosis: fibroblasts and myofibroblasts

A.2.1 Normal lung fibroblasts

Fibroblasts are a heterogeneous population of spindled morphology cells whose major functions are to maintain tissue homeostasis and regulate the turnover of ECM. Fibroblasts are also critical for proper wound healing. During normal wound healing, fibroblasts migrate to the site of injury, differentiate into myofibroblasts (α-SMA expression), secrete and assemble ECM, and contract wounds closed. During late stages of wound healing, normal myofibroblasts undergo apoptosis and the wound is resolved [Kalluri 2006]. However, in IPF, myofibroblasts persist and accumulate in the airways eventually leading to organ failure. Understanding how fibroblasts differentiate into pathological myofibroblasts is an important question in the field.

A.2.2 The myofibroblast in Idiopathic Pulmonary Fibrosis

It is useful to conceptualize the IPF myofibroblast using a cancer paradigm. Although not driven by somatic mutations, the IPF myofibroblast shares several hallmark characteristics with cancer that distinguishes it from other fibroblasts in the lung. Henke's research group has shown that IPF myofibroblasts differ from normal fibroblasts as they have an increase Akt-signaling pathway which is mediated by suppressed expression of PTEN and caveolin-1 which are negative regulators of the Akt pathway [Xia 2008]. With this pathologically active growth signaling axis, IPF myofibroblasts resist the negative

proliferative regulation type I collagen has while resisting apoptosis. This supports the increased proliferation and decreased apoptosis branch of the hallmarks of IPF (**Figure A.1**).Other mechanistic studies have shown that IPF myofibroblasts resist apoptosis through lower levels of prostaglandin E2 generator cyclooxygenase 2 (COX-2 – apoptosis-inducing) [Wilborn 1995] and lower levels of fork-head box- O3a (FoxO3a – apoptosis-inducing) [Nho 2013]. Myofibroblasts are effector cells in IPF and are characterized by their expression of alpha smooth muscle actin (αSMA) and up-regulation of ECM synthesis versus non-activated fibroblasts. IPF myofibroblasts have activated fibroblast characteristics: increased αSMA and increased type I collagen expression versus control lung fibroblasts [Khalil 2015, Xia 2014]. IPF fibroblasts, as compared to control lung fibroblasts, form fibrotic lesions in xenograft zebrafish assays [Benyumov 2011] and xenograft mouse models [Xia 2014]. Lastly, the fibrotic reticulum formed in the IPF lung anatomically appears to represent invasive tumor-like lesions all of which justify the cancer paradigm terminology.

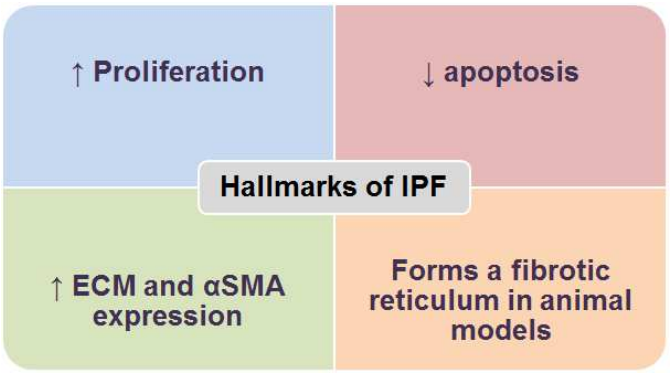

Figure A.1 Hallmarks of Idiopathic Pulmonary Fibrosis. IPF myofibroblasts have an increased Akt – signaling growth axis which leads to increased proliferation and decreased apoptosis. IPF myofibroblasts have activated fibroblast phenotypes (increased αSMA expression) and increased ECM synthesis which is an effector cell in IPF. Lastly, IPF myofibroblasts form fibrotic reticulum in zebrafish and rodent models.

Chapter A.3. The biology of pathological extracellular matrix: a role for fibroblast-to-myofibroblast differentiation

Each organ consists of a highly structured ECM tuned to the specific function of that organ. Maintenance of ECM homeostasis is critical for regulating biochemical signals that support cellular functions including attachment, differentiation, growth, and survival [DuPort 2011]. However, during pathological remodeling of the ECM that occurs in cancer and fibrosis, ECM homeostasis is compromised [Humphrey 2014]. It is therefore important to understand the extent to which pathological cellular functions in disease are ECM-mediated and –supported. Below are ways that pathological ECM cause fibroblast-to-myofibroblast differentiation.

A.3.1 TGF-beta mediated myofibroblast differentiation

Transforming growth factor beta (TGF-β) is an abundant growth factor embedded in the pathological ECM in IPF. TGF-β is a cytokine that inhibits proliferation and induces apoptosis of epithelial cells [Leask 2004]. In fibroblasts, TGF- β mediates myofibroblast differentiation, proliferation, and increased ECM synthesis through SMAD downstream targets [Hu 2003, Hinz 2012]. TGF-β

signaling in fibroblasts is one mechanism by which a profibrotic ECM mediates myofibroblast differentiation (**Figure A.2**).

A.3.2. Pathological stiffness mediated myofibroblast differentiation

IPF lungs are an order of magnitude stiffer than control lungs [Booth 2012], and stiffness drives myofibroblasts differentiation independent of TGF-β [Huang 2012, Lui 2014]. Using polyacrylamide hydrogels (PA gels) simulating IPF stiffness, Huang et al. showed that through a ROCK/RhoA – MLK1 mechanotransduction signaling axis, myofibroblast differentiation is achieved in primary lung fibroblasts on hydrogels simulating IPF stiffness. Liu et al. showed that PA gels of IPF stiffness directed myofibroblast differentiation and collagen expression in a Yes-associated protein (YAP) dependent manner [Liu 2014]. Increased matrix stiffness is another mechanism by which a profibrotic ECM mediates myofibroblast differentiation (**Figure A.2**).

A.3.3. ECM mediated myofibroblast differentiation

IPF tissue is compositionally different than normal lungs. As myofibroblasts populate the lung, they deposit a type I collagen rich ECM. Booth et al. was the first group to use decellularized lung ECM from control or IPF patients (Ctrl- or IPF ECM) as a scaffold for cells to adhere and interact. They identified that IPF-ECM directs fibroblast-to-myofibroblast (increased αSMA expression) differentiation in a TGF-β-independent manner [Booth 2012]. Pathological ECM components, such as Fibronectin-EDA (abundant in IPF and

low in normal lung), has also been shown to drive myofibroblast differentiation of primary fibroblasts [Bhattacharyya 2014]. Pathological ECM composition is another mechanism by which a profibrotic ECM drives myofibroblast differentiation (**Figure A.2**).

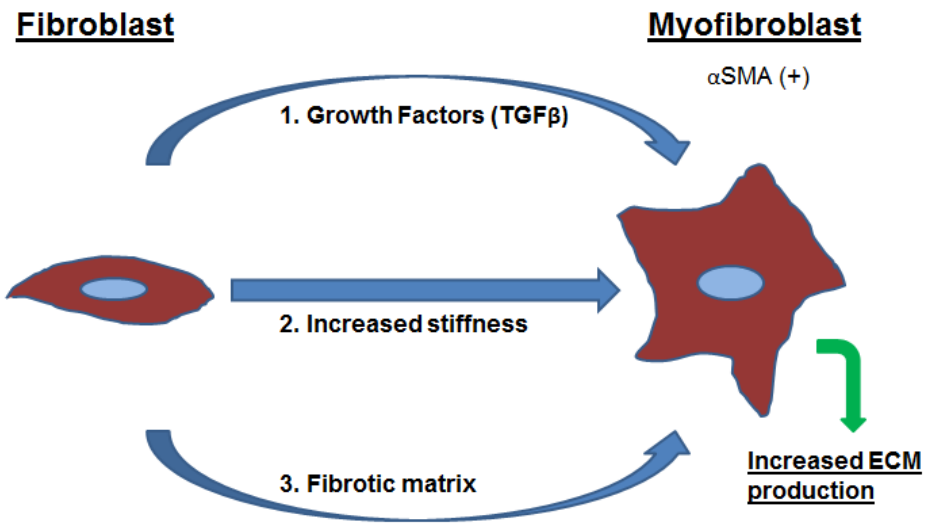

Figure A.2. Myofibroblast differentiation driven by a profibrotic environment. IPF is enriched with growth factors such as TGF-β, is an order of magnitude stiffer, and compositionally different than control lungs. These factors drive fibroblast differentiation into myofibroblasts (increased αSMA expression) which are effector cells in IPF that increase ECM production.

Myofibroblast differentiation has been widely studied, and the mechanism of increased ECM production has been under intense research. Using single parameters of pathological ECM mediated myofibroblasts differentiation has given us insight into the mechanism of myofibroblast activation. What is less

explored is the mechanism by which pathological ECM modulates ECM expression in myofibroblasts.

A.4. MicroRNA-29 deregulation in Idiopathic Pulmonary Fibrosis

A.4.1. MicroRNA biogenesis

MicroRNAs are small non-coding RNAs of ~22 nucleotides that post-transcriptionally modulate gene expression. To date, there are about 2,588 microRNAs encoded in the human genome [Ha 2014]. A unique feature of microRNAs is that they are often clustered in operons and expressed polycistronically. However, each microRNA in that cluster can be differentially regulated at the level of microRNA processing [Mott 2013] suggesting higher orders of microRNA regulation.

MicroRNA's are transcribed by RNA polymerase II (Pol II) into what is called the primary microRNA (Pri-miR) that is fully equipped with a 5' cap and poly-A tail (over 1kb in size). Pri-miR's contain stem loop secondary structures that are recognized by microprocessing complex (Drosha, DGCR8, and others) that cleave the junction between the stem loops and form the precursor microRNA (Pre-miR). Pre-miR is exported from the nucleus to the cytoplasm via exportin 5 where it is recognized by Dicer and further processed into a small RNA duplex. AGO proteins bind the RNA duplex, unwind, trim, and load a mature strand in concert with other protein components to form the RNA-induced silencing complex (RISC). Mature microRNA's are classified by their seed sequences (~8 nucleotides) that give them specificity to their target mRNAs.

Mature RISC complexes bind target mRNA's and direct its translational repression or mRNA cleavage (**Figure A.3**)

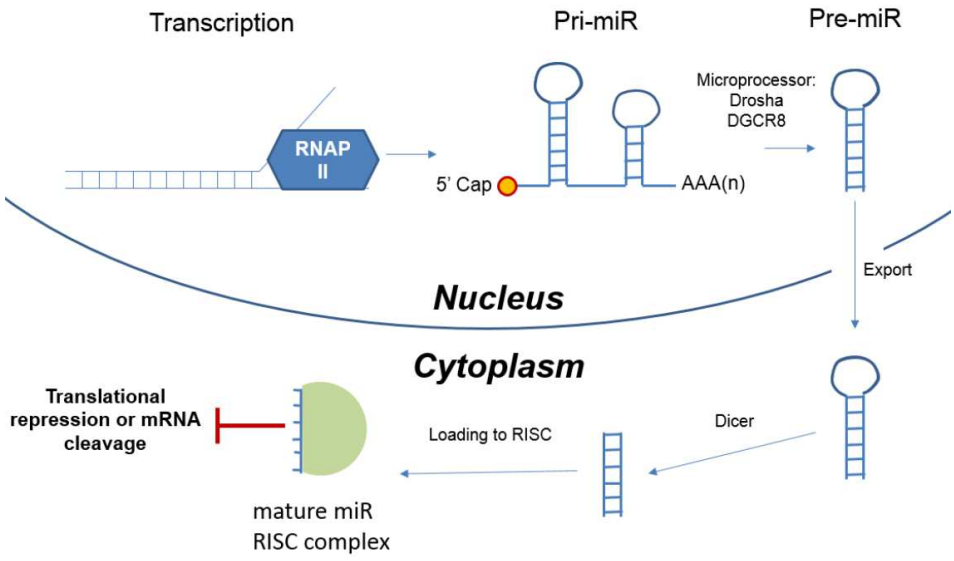

Figure A.3. MicroRNA biogenesis: MicroRNA's are transcribed in the genome via RNA polymerase II (Pol II) into primary microRNA (Pri-miR) that are 5' capped and contain a poly-A tail. Pri-miR's are further cleaved into precursor microRNA (pre-miR) via the microprocessor complex and finally exported from the nucleus to the cytoplasm. In the cytoplasm, Dicer processes Pre-miR into a small RNA duplex that is loaded onto the RNA-induced silencing complex (RISC) where it can bind target mRNA's and cause translational repression or mRNA cleavage.

A.4.2 MicroRNA regulation

It is of interest to understand microRNA regulation since 60% of our protein encoding mRNA's contain at least one known microRNA target sequence. It is therefore not surprising that microRNA's are tightly regulated at

the levels of transcription and post-transcription. I will focus my efforts on post-transcriptional regulation as transcriptional regulation is unique to each microRNA's promoter region and under Pol II regulatory components.

MicroRNA post-transcriptional regulation occurs at different stages: nuclear processing and cytoplasmic processing. The microprocessor complex (Drosha and DGCR8) is essential for nuclear processing of Pri-miR to Pre-miR. Drosha deletion is lethal in mice [Chong 2010] and DGCR8 deletion arrests mouse development [Wang 2007]. The expression of these components are crucial for proper microRNA biogenesis, however there are a variety of post modifications that effect Drosha and DGCR8's stability, nuclear localization, and processing activity. For instance, phosphorylation of Drosha by GSK3β at serine 300 and serine 302 drives Drosha nuclear localization [Tang 2010 and Tang 2011], while acetylation of Drosha in its N-terminus competes for ubiquitination, hence increases Drosha stability [Tang 2013]. Similarly, DGCR8 processing activity is increased by HDAC1 deacetylation of critical lysine residues used for RNA binding [Wada 2012]. Phosphorylation of DGCR8 by ERK enhances protein stability [Herbert 2013] (**Figure A.4a**).

The microprocessor complex also includes RNA helicase (DEAD-box containing – DDX) proteins whose functions are to enhance processing activity. p68 (DDX5) and p72 (DDX17) have been shown to be upregulated in breast, prostate, and colon cancer [Van Kouwenhove 2011]. Either p68 or p72 knockout in mice are lethal, as studies show that they are required for microRNA processing from Pri-

miR's [Fukuda 2007]. The tumor suppressor, p53, has been shown to interact with p68 and enhance microRNA processing activity, and cancer-driving p53 mutants have been shown to decrease p68 interaction and decrease mature microRNA abundance that function in growth suppression [Suzuki 2009]. SMAD signaling through TGF-β has also been shown to associate with p68 and increase microRNA processing [Davis 2008]. The hippo pathway's effector protein, Yes-associated protein (YAP) has been shown to bind and sequester p72 which alters global microRNA processing [Mori 2014] (**Figure A.4a**).

Nuclear export of microRNA's depends on a transport complex containing exportin-5 and RAN-GTP. This complex binds Pre-miR's, and hydrolyses GTP in order to translocate Pre-miR's through nuclear pores into the cytosol. Although this complex is not well understood, mutations in exportin-5 has been discovered in transformed cell lines that lead to global microRNA suppression [Melo 2010]. Cytoplasmic Pre-miR processing is performed by Dicer. Dicer recognizes and cleaves Pre-miR's near the stem loop, releasing a small RNA duplex. Dicer is regulated by its cofactor, TAR RNA-binding protein (TRBP), which modulates Dicer processing efficiency. Although TRBP is not essential for Dicer-mediated Pre-miR processing [Lee 2006], TRBP2 is mutated in transformed cells which leads to reduced Dicer stability [Melo 2009]. TRBP phosphorylation by ERK has also been shown to modulate growth promoting microRNA up-regulation [Paroo 2009] (**Figure A.4b**).

Small RNA duplexes that are released from Dicer are loaded onto argonaute proteins (AGO1-4). AGO proteins selectively bind small RNA duplexes according to their structural and chemical properties, and unwind the RNA duplex by selecting the most thermodynamic stable end of the RNA duplex [Ha 2014]. Gene silencing by AGO proteins is achieved in processing bodies (P – body) and AGO stabilization and P – bodies retention is influenced by post-transcriptional modifications. AGO is hydroxylated by type I collagen prolyl 4-hydroxlase (4PH) which increases AGO2's stability and P – body localization [Qi 2008]. Phosphorylation of AGO2 by AKT3 leads to P – body localization [Horman 2013] (**Figure A.4b**).

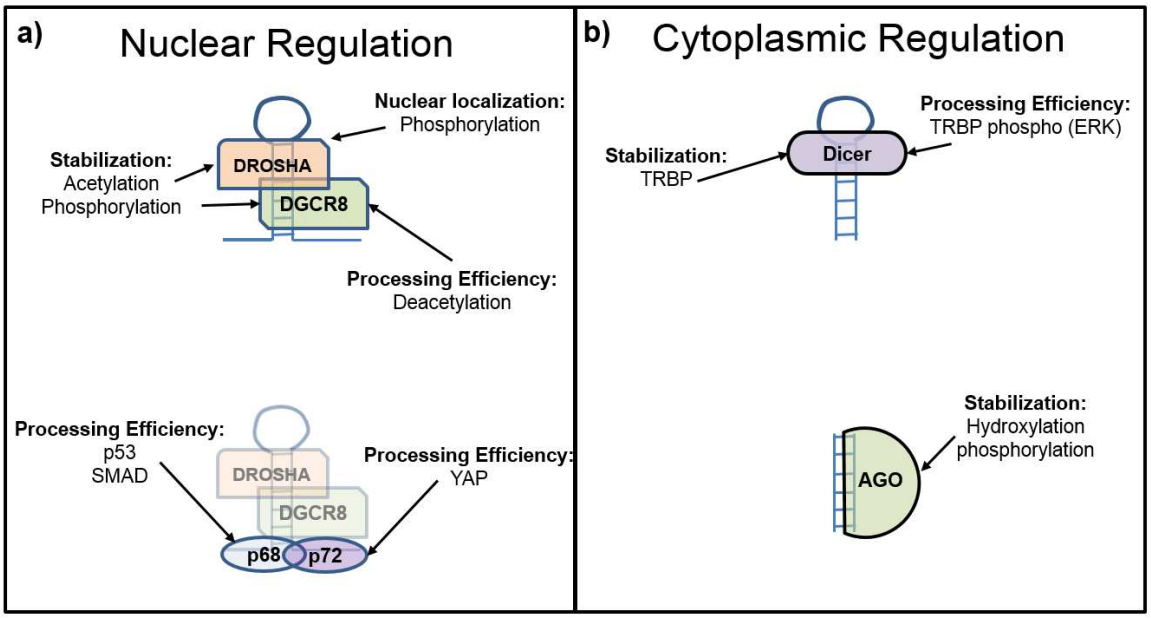

Figure A.4. MicroRNA nuclear and cytoplasmic regulation: Once microRNA's are transcribed, they're subjected to processing regulation. a) Drosha and DGCR8 form a microprocessor complex and mediate cleavage of the Pri-miR, leaving the stem loop. Drosha and DGCR8

undergo a variety of post-transcriptional modifications that affect its stability, nuclear localization, and processing efficiency. DEAD-box RNA helicases (p68 and p72) are cofactors that bind single stranded RNA at the stem interface and mediate processing efficiency and are subject to cellular signaling that modulate processing activity. b) Dicer protein nicks the translocated Pre-miR at the stem loop interface. Dicer is regulated by other RNA binding proteins to either stabilize or modulate processing efficiency. AGO protein binds the small RNA duplex and is also subjected to post-transcriptional modification to effect microRNA stabilization and localization of AGO.

Mature microRNA decay is not understood. When associated with RISC, microRNA ends are protected by AGO protein binding making it difficult for microRNA decay to occur [Ha 2014]. However, one mechanism for degrading Pre-miR has been unraveled: RNA-editing. Let-7 precursor microRNA recruits a terminal uridylyl transferase (TUT4) to induce oligouridylation of precursor Let-7's 3' end. The addition of an oligo-U tail prevents Dicer processing and leads to microRNA degradation [Heo 2008]. Poly (A) polymerase, GLD-2, has been shown to selectively target miR-122 and add an adenosine to the 3' end. This single edit was shown to stabilize miR-122 which is another example of RNA-editing affecting microRNA stability [Katoh 2009]. Although microRNA turnover is nuclease mediated, the mechanism of regulation is largely unknown and a challenge in the field.

A.4.3. MicroRNA-29: a profibrotic regulator of pathological extracellular matrix

Myofibroblasts increase ECM production, and one mechanism of ECM up-regulation is mediated by the suppression of microRNA-29 (miR-29) which is

suppressed in IPF [Oak 2011, Parker 2014, Khalil 2015]. MiR-29 is of great interest as its target genes are ECM, integrin, and ECM modifying genes (**Figure A.5a**) [Cushing 2011, Parker 2014]. MiR-29 targets a variety of ECM genes including collagen type I, III, IV, V, and laminin α1, α3, β3. Type I and type III collagen are abundantly found in IPF matrix and the receptors used to bind these are integrin's α2 and α11 (both of which are miR-29 targets). Finally, miR-29 targets ECM modifying genes that are critical in ECM turnover (MMP2 and MMP14) and important in ECM stiffening through crosslinking enzymes (LOXL2, **Figure A.5a**). MiR-29 is a profibrotic regulator as its suppression increases ECM production, allows attachment to fibrotic ECM by increasing integrin expression, and causes stiffening/crosslinking of fibrotic ECM.

A.4.4. MicroRNA-29 regulation

Mir-29 suppression is not unique to IPF, and has also been shown to be suppressed in fibrosis of the heart, kidney, and liver [He 2013]. Xiao et al. demonstrated that overexpression of miR-29 in a bleomycin-induced model of pulmonary fibrosis ablates the initiation of fibrosis [Xiao 2012]. Therefore, it is of great importance to understand how miR-29 is regulated in IPF.

The miR-29 family consists of 4 precursors: miR-29a, -29b-1, -29b-2, and -29c; miR-29b-1/a and miR-29b-2/c are expressed polycistronically and are encoded on chromosome 1 and 7, respectively. It is important to note that miR-29b-1 and miR-29b-2 are identical, and to date, there is no evidence of polymorphisms associated with miR-29. However, miR-29 has been shown to be

transcriptionally regulated by c-Myc, hedgehodge, NF-κB, TGF-beta, YAP, PP2A/HDAC4, and Erk/c-Fos (**Figure A.5b**) [Mott 2013, Wang 2008, Qin 2011, Khalil 2015, Tumaneng 2012, Chen 2012]. Although these research groups used different cell types and different systems, it is important to understand how miR-29 is regulated in models of fibrosis.

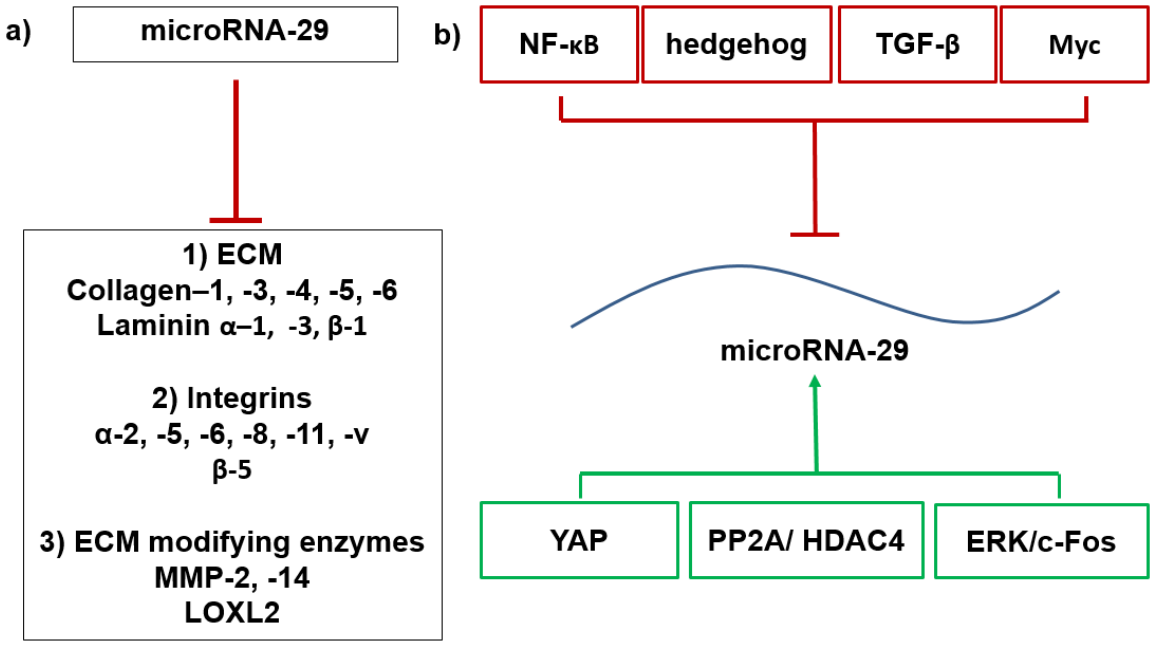

Figure A.5. MicroRNA-29 gene targets and transcriptional regulation. a) MicroRNA-29 is a fibrotic regulator and genome studies have shown that targets of miR-29 are ECM, integrin, and ECM modifying enzymes. b) MiR-29 transcriptional regulation has been extensively studied and research has shown that miR-29 is transcriptionally suppressed by NF-κB, hedgehog, TGF-β, and Myc. MiR-29 has been shown to be transcriptionally activated by YAP, PP2A/HDAC4, and ERK/c-Fos.

A.4.5 MicroRNA processing deregulation in Idiopathic Pulmonary Fibrosis.

MicroRNA global suppression is a characteristic of cancer, and microRNA deregulation is a theme in IPF pathogenesis [Oak 2011, Kusum 2015]. Oak et al. was the first to report a global deregulation of microRNA expression in IPF. In this study, they evaluated 88 of the most highly expressed microRNA's and determined that 36 microRNA's were significantly decreased (including miR-29a, -29b, and -29c) and 11 microRNA's were significantly increased *ex vivo*. They also quantified, by PCR, relative expression of AGO1 and AGO2 and found lower expression in IPF fibroblasts. They conclude that the progression of IPF might be due to aberrant microRNA processing. This therefore motivates us to study how miR-29 is regulated in the context of fibrotic ECM.

A.5. Modeling Pathological ECM

A.5.1 Physiological versus pathological decellularized ECM: Pathological ECM regulates miR-29 expression

Booth et al. was the first to decellularize control and IPF lung tissue (Ctrl-ECM and IPF-ECM) and show that IPF-ECM is an order of magnitude stiffer, and compositionally different than Ctrl-ECM. Their manuscript outlines an innovative methodology paper and their studies show that when primary lung fibroblasts are cultured on IPF ECM, these fibroblasts differentiate into myofibroblasts. To further unravel how ECM directs IPF characteristics, our group took a genome-wide approach to identify transcriptome and translatome profiles. We found that IPF-ECM drives ECM gene translational activation [Parker 2014]. We identified that miR-29c was suppressed by IPF-ECM while restoration of miR-29c ablated

ECM gene translational activation (**Figure A.6**). These studies highlight the use of authentic decellularized ECM as a model to study IPF pathogenesis. However, the mechanism of miR-29 suppression is not completely understood.

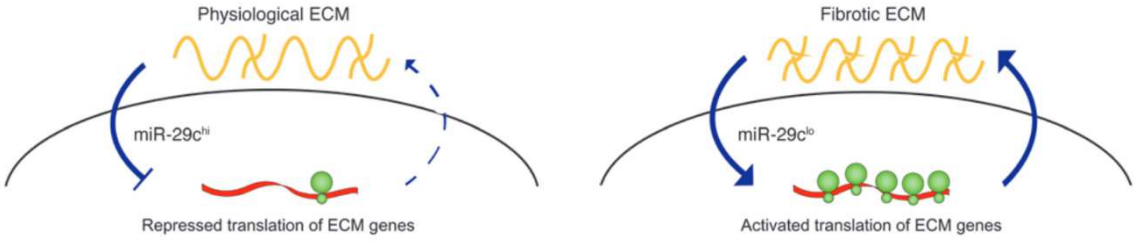

Figure A.6. Fibrosis begets fibrosis. IPF-ECM activates the translation of ECM genes in primary lung fibroblasts through the inhibition of microRNA-29, while control ECM suppresses the translation of ECM genes via the increase of microRNA-29. IPF-ECM constitutes a positive feedback loop that amplifies ECM gene expression and allows for the contiguous spread of fibrosis.

A.5.2 Polyacrylamide Hydrogels to Model Composition and Stiffness

Polyacrylamide hydrogels (PA gels) are conveniently used to model stiffness as a range of stiffness's can be accomplished by adjusting acrylamide concentrations. PA gels are then coated with a monolayer of any ECM-derived protein to study cell – ECM interactions [Cretu 2010] **(Figure A.7**). When cultured on PA gels simulating IPF stiffness, lung fibroblasts become activated in a YAP/TAZ dependent manner [Liu 2014]. They differentiate into myofibroblasts [Huang 2012], generate increased force and manifest an increased rate of proliferation [Marinković 2013]. These studies demonstrate that stiffness drives fibroblast into IPF-like fibroblasts and serve as a valuable model to study IPF

pathogenesis. However, no one has yet to report the role of stiffness and miR-29 expression.

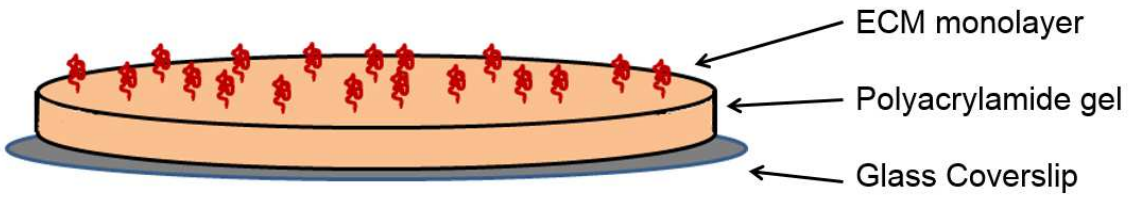

Figure A.7. Polyacrylamide Hydrogels. Polyacrylamide hydrogels can be modulated to simulate stiffness's seen in normal and IPF lungs. Polyacrylamide hydrogels of IPF stiffness has been shown to drive many fibrotic characteristics. The diversity of this assay allows researchers to coat a monolayer of any ECM protein to determine effects of stiffness and a variety of compositions.

A.6 Conclusions

The hallmark characteristics of IPF resemble many also used to define cancer. Because there are no animal models that can fully recapitulate IPF, creative ways to model disease progression such as modeling pathological ECM has been in the spotlight. Mechanisms regulating ECM synthesis, such as microRNA-29 regulation, have been of high interest to begin uncoupling the profibrotic response. Herein we aim to understand the relationship between pathological ECM and microRNA-29 regulation.

Chapter B: Pathological extracellular matrix regulates microRNA-29 at the level of microRNA processing in Idiopathic Pulmonary Fibrosis

B.1 Study Design

This dissertation is divided into three sections. The first is to (i) determine whether miR-29 is regulated by the mechanical property of stiffness. Second, (ii) to determine at which level of regulation miR-29 is controlled, and finally, (iii) to identify the molecular mechanism by which IPF-ECM suppresses miR-29. The experimental study design and end points are shown in **Figure B.1**.

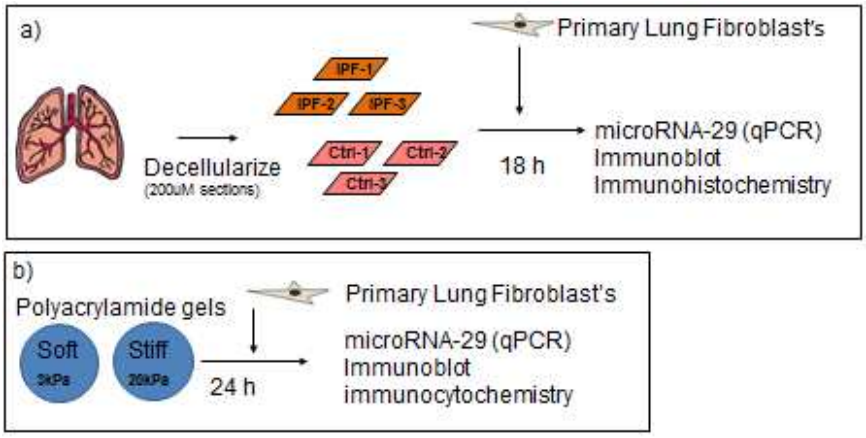

Figure B.1. Study Design. a) Human lungs from control or IPF patients were decellularized at 200 μM sections of approximately 1cm^2 in size. To control for patient variability, we pooled ECM from 3 patients (either control or IPF) per reaction and cultured ECM with 5 x 10^5 fibroblasts for 18 hours in 1% serum. B) Polyacrylamide gels of physiological stiffness (Soft – 3kPa) or IPF stiffness (Stiff – 20 kPa) were made and seeded with 2 x 10^5 fibroblasts for 24 hours in 1% serum. At the end of the experiments, total RNA is isolated for quantitative PCR, protein for immunoblots, or formalin-fixed for histological analysis.

B.2 Materials & Methods

Primary human lung fibroblast lines and culture conditions: All studies involving patient derived material were approved by the University of Minnesota

IRB. De-identified human lung tissue was obtained from the University of Minnesota Tissue Procurement Facility. All cell lines were derived from histologically uninvolved tissue adjacent to resected tumors. Tissue was minced and added to 35mm plastic tissue culture dishes for 2-3 weeks in explant growth medium (DMEM + 20%FBS, 200 IU/mL Streptomycin, 200 IU/mL Penicillin). Outgrowth cells were sub-cultivated into 150-mm dishes in fibroblast growth media (DMEM + 10%FBS, 100 IU/mL Streptomycin, 100 IU/mL Penicillin) and designated passage 1. Cells were characterized as fibroblasts by their typical spindle shaped morphology, the expression of vimentin and alpha smooth muscle actin and no expression of factor VIII and surfactant C. Cells were cultured (37^{o}C, 5% CO_2) in fibroblast growth medium and sub-cultivated at a 1:3 split ratio. All experiments were conducted with cells between passages 3 to 6.

Decellularized human lung ECM: Human lung tissue was obtained from the University of Minnesota's Tissue Procurement Facility as histologically uninvolved tissue adjacent to resected tumor, or from patients clinically confirmed as IPF at time of biopsy, lung transplant or autopsy, following a protocol approved by the University of Minnesota's Institutional Review Board of Human Subjects Research. Freshly frozen tissue was sectioned at 200μM and decellularized in a series of solutions (1%SDS, 1% Triton X-100, 1M NaCl, DNase) as described [Parker 2014]. Cells ($5x10^5$) were added to 15mL conical polypropylene tubes oscillated at ~6-8 revolutions per minute. Each tube contained three control or three IPF decellularized ECM sections (1cm by 1cm),

2mL survival medium (DMEM + 1% FBS, 100 IU/mL Streptomycin, 100 IU/mL Penicillin) and were incubated at 37^{o}C in an atmosphere containing 5% CO_2.

Polyacrylamide Gels: Polyacrylamide gels of 3 kPa or 20 kPa were cast following an established protocol (Cretu 2010). As indicated in the text, gels were coated with either 100µg/mL Type I Collagen (Advanced BioMatrix 5005), 50 µg/mL Type III Collagen (Advanced BioMatrix 5021), 10 µg/mL Fibronectin (Advanced BioMatrix 5050), or a combination of all three using 10 µg/mL of each. 2 x10^5 fibroblasts were seeded on each gel and incubated in survival medium.

Vectors/Plasmids: pQCXIH-Flag-YAP-S127/381A and pQCXIH-Myc-YAP-5SA were obtained from Addgene (plasmid # 33069 and plasmid #33093) and FLAG-YAP-S127/381A and Myc-YAP-5SA were cloned into GIPZ lentiviral systems (GE Healthcare). Cells were transduced and used for experimentation after 48 hours. YAP knockdown was achieved by using GIPZ lentiviral systems (GE Healthcare, V2LHS-65508), and transduced cells were used after 72 hours.

Western blot and antibodies: Cells were lysed by addition of Lysis Buffer [150 mM NaCl, 1 mM EGTA, 50 mM Tris, pH 7.4, 1% Triton X-100, 1% Nonidet P-40, 1% sodium deoxycholate, with protease inhibitors (Roche 11873580001)] to polyacrylamide gels or ECM. Blots were incubated (4^{o}C) overnight with primary antibodies: rb anti-YAP (cell signal 14074; 1:2000), (Cell signal 13008; 1:2000), rb anti-GAPDH (Santa Cruz Bio sc-25778; 1:2,000), and rb anti-αSMA (Abcam ab-32575; 1:2,000). Blots were washed (describe) and incubated (1 h, room temperature) with secondary antibodies (either goat anti-rabbit IgG HRP

(Calbiochem 401393; 1:10,000) or Rat anti-mouse IgG HRP (Calbiochem 401253; 1:2,500). Blots were developed using ECL western blotting detection (GE Healthcare W9488333) following the manufacturer's protocol).

Reverse Transcription and Quantitative PCR Analysis: RNA was isolated with TRI reagent (Sigma T9424) and chloroform extracted. Isolated RNA was reverse transcribed using miScript II RT Kit (Qiagen 218161) according to the manufacturer's recommendation. Qiagen simplifies PCR by using validated primers which are all set at the same PCR conditions. Using SYBR – Green PCR Kit (Qiagen 218073; manufacturers recommendation), mature microRNA-29-a, -b, -c, 214, or RNU6 validated primers (Qiagen MS0003262, MS00006566, MS00003269, or MS00033740 respectively) and precursor microRNA-29-a, -c, 214, GAPDH, CTGF, CYR61, YAP, or RRN18S validated primers (Qiagen MP00001736, MP00001757, MP00001540, QT00079247, QT00052899, QT00003451, QT00080822, or QT00199367 respectively) were used for qPCR and analyzed by Roche Light Cycler 1.5 (Software Version 3.5). Primary mir-29a, are established primers (Mott 2010): forward 5'-CAGAGACTTGAGCATCTGTG, reverse 5'-AACCGATTTCAGATGGTG and used as described.

Luciferase Assay: The miR29-b-1/a firefly luciferase promoter construct was a kind gift from Dr. Justin Mott, University of Nebraska [Mott J 2010]. The microRNA processing assay luciferase construct was a kind gift from Dr. Richard Gregory, Harvard Medical School [Mori 2014]. Plasmids miR29-b-1/a and pRL-TK (Promega E2241) or microRNA processing construct were transfected using

Lipofectamine 3000 (Life Technologies L3000008) according to the manufacturer's recommendation. Using a dual luciferase reporter assay (Promega E1910), luminescence was quantified using a Lumat LB 9507 luminometer (Berthold Technologies).

BrdU labeling: Fibroblasts cultured on decellularized lung matrices were incubated with BrdU (Life Technologies 00-0103; manufacturer's recommendation) for 24 hours.

Immunohistochemistry/Immunofluorescence: Fibroblasts on decellularized lung ECM and human lung samples were formalin-fixed and paraffin-embedded (FFPE). De-paraffinized and rehydrated 4 μm sections were subjected to antigen-heat retrieval (BioCare RV1000) for 25 minutes at 100^{o}C followed by 3% hydrogen peroxide and a Background SNIPER (BioCare BS966) blocking reagent. Fibroblasts on polyacrylamide gels were formalin-fixed and subjected to antigen retrieval followed by a Background SNIPER blocking reagent. For anti-pro-collagen type I antigen retrieval we used proteinase K (Millipore 21627; working strength) for 10 minutes instead of antigen-heat retrieval. Sections and gels were exposed overnight (4^{o}C) to primary antibodies diluted in 10% Background SNIPER. Primary antibodies: rb anti-YAP (Cell Signal 14074; 1:200), rat anti-human procollagen type I (Abcam 64409; 1:500), and mouse anti-BrdU (Roche 11903800; 1:400). For permanent stain, biotin-conjugated secondary antibody (Covance SIG-32236; working strength) was applied followed by Streptavidin-HRP (Covance SIG-32254; working strength) and developed with

DAB chromagen (Covance SIG-31042; manufacturer's recommendation). Slides were counterstained with hematoxylin. For immunofluorescence, after overnight antibody incubation, anti-Rb Cy3 (Jackson 711-165-152; 1:500) was reacted in 10% Background SNIPER and coverslipped with mounting media containing DAPI (Invitrogen P36931).

Histological Imaging: Samples containing permanent stains (H&E, DAB substrate/hematoxylin counterstain) were imaged using a Leica EC3 microscope and Leica MME camera. Fluorescent images were collected using a Zeiss Axiovert 200 fluorescent microscope and analyzed using AxioVision (Release 4.7.2).

Statistics and Graphs: All graphs where made using Excel, and a Student T-Test or Student Paired Tests were performed as appropriate. All error bars are represented as standard errors of the mean and asterisks indicate a p-value < 0.05.

B.3 Results

B.3.1 ECM stiffness does not account for the regulation of microRNA-29 by IPF-ECM

We have previously shown that IPF-ECM suppresses miR-29c with a trend toward suppression of miR-29a and miR-29b [Parker 2014]. We reexamined this effect with methodological revisions designed to maximize the impact of the ECM, minimize the effect of serum growth factors, and control for patient to patient lung ECM heterogeneity (**Figure B.2**). When primary lung

fibroblasts were cultured in low-serum survival media on pooled lung ECM (3 Ctrl-ECM preparations or 3 IPF-ECM preparations in each reaction), we observed a significant decrease of all 3 miR-29 species (**Figure B.3**).

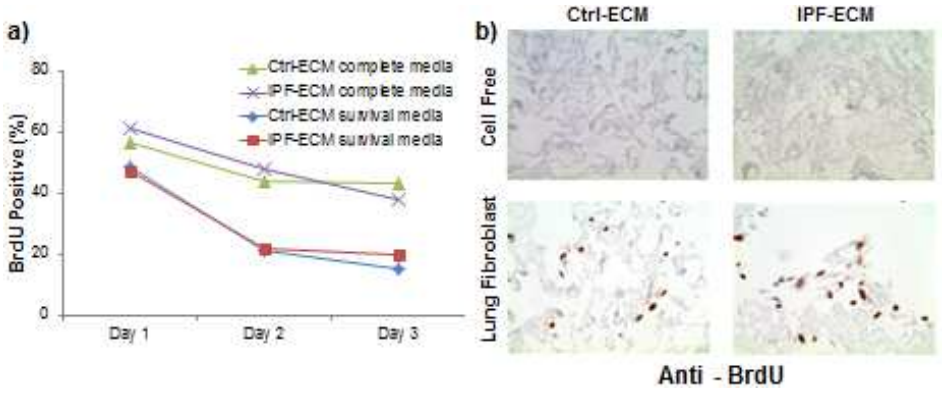

Figure B.2: Lung fibroblasts survive and proliferate on Ctrl- or IPF-ECM. Lung fibroblasts cultured in either survival or complete medium were pulsed with BrdU for 24 hours and formalin-fixed paraffin embedded. a) 3 day time-course of percent BrdU positive cells, b) representative images of ECM on day 3 with (lower panels) or without (upper panels) fibroblasts (n = 1).

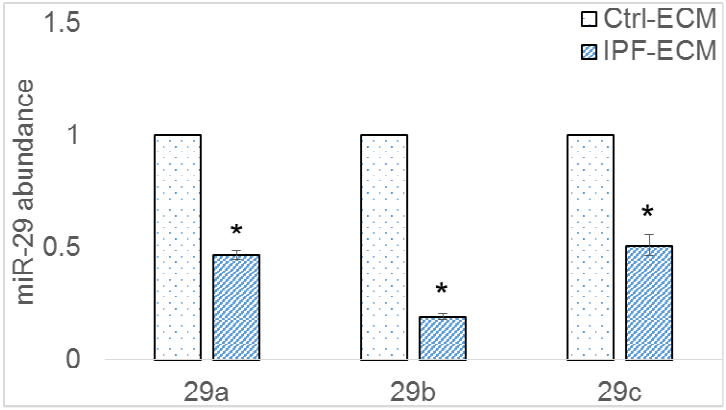

Figure B.3: IPF-ECM suppresses microRNA-29 expression: Lung fibroblasts were cultured on Ctrl- or IPF-ECM for 18 hours and mature miR-29 -a, -b, and -c were quantified by qPCR. Expression was normalized to RNU6 (n = 3).

IPF lungs are an order of magnitude stiffer and compositionally different than control lungs [Booth 2012]. When cultured on PA gels simulating IPF stiffness, lung fibroblasts become activated in a YAP/TAZ dependent manner [Liu 2014]. They differentiate into myofibroblasts [Huang 2012], generate increased force and manifest an increased rate of proliferation [Marinković 2013]. In order to determine whether stiffness and/or composition could account for our observations of miR-29 on decellularized ECM, we first cultured lung fibroblasts on synthetic polyacrylamide hydrogels (PA gels) of physiological stiffness (Soft – 3 kPa) or IPF stiffness (Stiff – 20 kPa) coated with type I collagen and measured mature miR-29 abundance. In accord with published data, lung fibroblasts increased αSMA expression on stiff PA gels (**Figure B.4**). Surprisingly, mature miR-29 was up-regulated by stiff PA gels (**Figure B.5a**). The PA gel system is versatile as it allows the gels to be coated with any matrix-derived protein of interest [Cretu 2010]. To test the relative importance of stiffness versus composition in regulating mature miR-29 abundance, we coated PA gels with type III collagen alone, fibronectin alone, or an equal ratio of type I collagen, type III collagen, and fibronectin and measured mature miR-29 abundance (**Figure B.5b - d**). Our results show that stiffness up-regulates mature miR-29 abundance, independent of composition. This excludes the possibility that any single integrin/ECM receptor can account for the miR-29 regulation we observed on decellularized lung ECM. It also makes it unlikely that ECM stiffness is the primary driver in IPF-ECM.

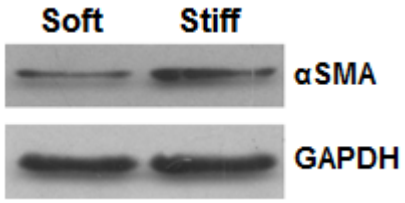

Figure B.4: Stiffness upregulates αSMA expression in lung fibroblasts. Lung fibroblasts were cultured on soft or stiff PA gels for 24 hours and immunoblot was performed for αSMA and GAPDH. (n = 2, representative blot shown).

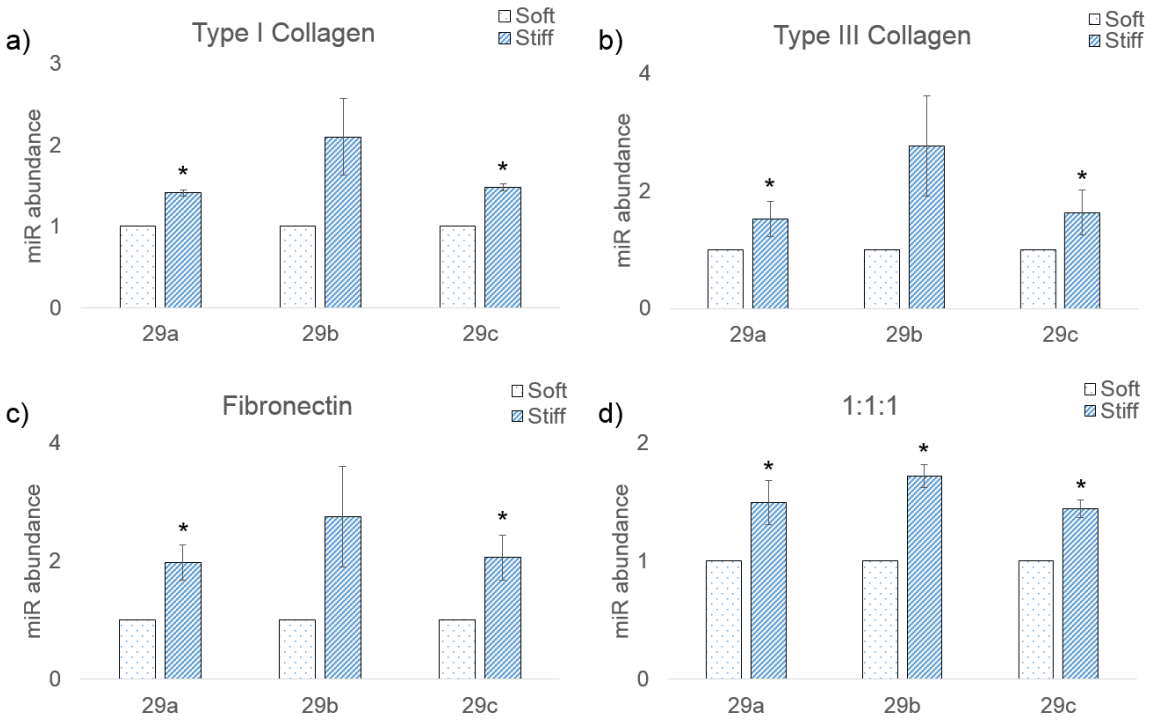

Figure B.5: Stiffness, not composition, regulates miR-29 expression. Primary lung fibroblasts were cultured on soft or stiff PA gels for 24 hours and qPCR was performed for mature miR-29a, -29b, and -29c (normalized to RNU6). PA gels were coated with either a) type I collagen, b) type III collagen, c) fibronectin, or d) a 1:1:1 ratio of type I collagen, type III collagen,

and fibronectin. (n = 3 independent replicates for figure 6a-c. n = 6 independent replicates for figure 6d).

B.3.2. IPF-ECM regulates microRNA-29 post-transcriptionally

Regulation of microRNA expression occurs at the level of transcription, processing, and turnover [Ha 2014]. To examine transcriptional regulation of miR-29, we introduced a miR-29b-1/a luciferase reporter [Mott 2010] into lung fibroblasts and cultured them on ECM (**Figure B.6a**). Although not statistically significant (p=0.109), miR-29 luciferase activity showed a trend towards suppression by IPF-ECM. MicroRNA processing occurs co-transcriptionally, and processing of primary microRNA's into precursor microRNA's are better predictors of mature microRNA abundance as opposed to transcriptional regulation alone [Conrad 2014]. To determine whether processing of miR-29 precursors were differentially regulated by ECM type, we measured both mature and precursor miR-29a and -29c abundance (**Figure B.6b**). This independent experiment reproduces our previous results in which mature miR-29a and -29c are low on IPF-ECM and we now report an increase of precursor miR-29a and -29c in lung fibroblasts cultured on IPF-ECM, indicating that IPF-ECM negatively regulates microRNA processing. Our experiments examining the effect of ECM type on miR-29 transcription and processing reveal a robust negative effect of IPF-ECM on miR-29 abundance.

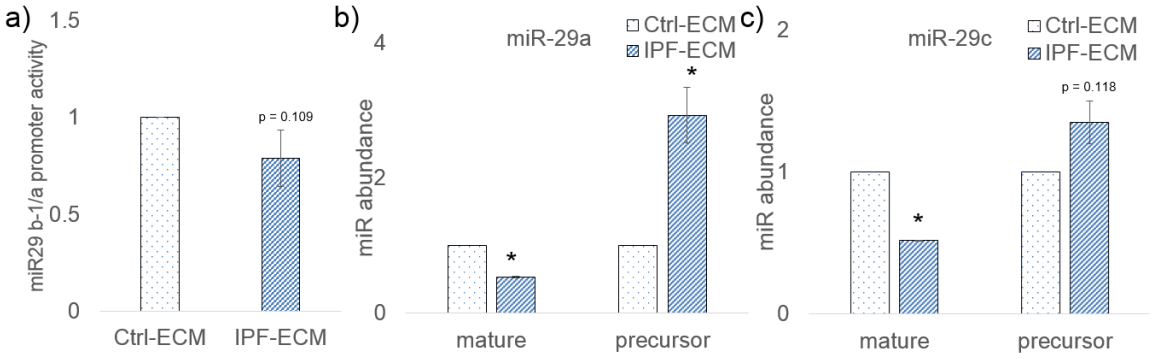

Figure B.6: IPF-ECM regulates microRNA-29 post-transcriptionally. a) miR-29 b-1/a firefly luciferase reporter was introduced into lung fibroblasts and cultured on Ctrl- or IPF-ECM for 24 hours. Activity was measured as firefly luciferase normalized to renilla luciferase (n = 5 independent replicates). b) Lung fibroblasts were cultured on control or IPF-ECM for 18 hours and mature and precursor microRNA was measured. Left panel is miR-29a and right panel is miR-29c (n = 2 independent replicates).

B.3.3. Hippo pathway is suppressed by IPF-ECM

Yes-associated protein (YAP), a transcriptional coactivator, is a downstream effector in the Hippo pathway and has been shown to drive fibrosis mediated by the mechanical property of stiffness [Liu 2015]. YAP has dual functions were YAP has been shown to up-regulate miR-29b-1/a transcription [Tumaneng 2012] and suppress global microRNA processing [Mori 2014]. We therefore sought to determine whether IPF-ECM increases YAP expression in correspondence with stiffness. When lung fibroblasts were cultured on IPF-ECM, YAP abundance was decreased (**Figure B.7a**). ECM type had only a modest impact on YAP mRNA levels (**Figure B.7b**) and had no significant effect on YAP translation (data not shown) [Parker 2014]. YAP stability is regulated by a series

of phosphorylation events that determine its proteosomal degradation [Zhao 2010]. When we inhibited the proteasome with MG132, the decrease in YAP abundance on IPF-ECM was ablated, indicating that YAP regulation by IPF-ECM occurs at the level of proteosomal degradation (**Figure B.7c**). As a transcriptional co-activator, YAP mediates its effect on gene expression in the nucleus. Immunohistochemical analysis indicated that YAP nuclear localization was reduced by IPF-ECM (**Figure B.7d**), along with expression of 2 canonical YAP transcriptional targets which served as a readout of YAP function (**Figure B.7e**). These results demonstrate that YAP is down-regulated by IPF-ECM in accord with a possible mechanistic relationship between YAP and IPF-ECM mediated down-regulation of miR-29 expression.

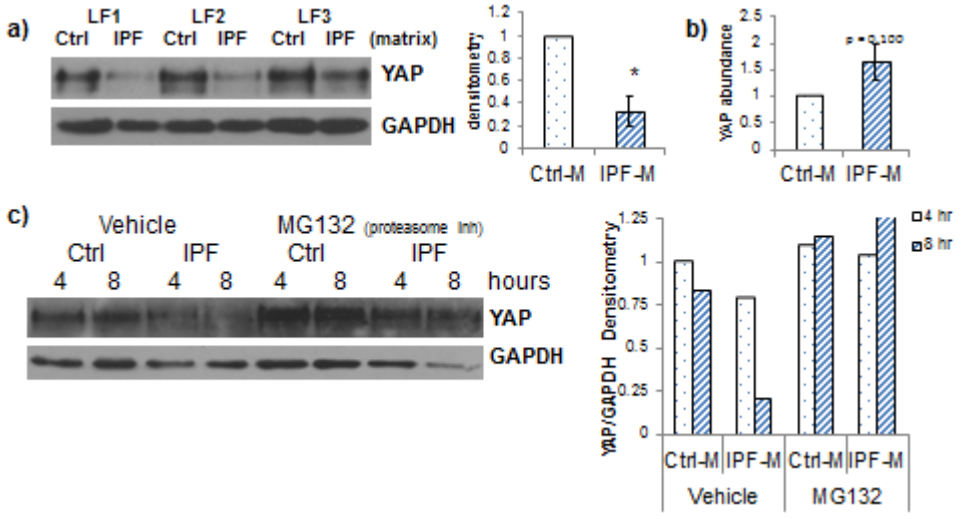

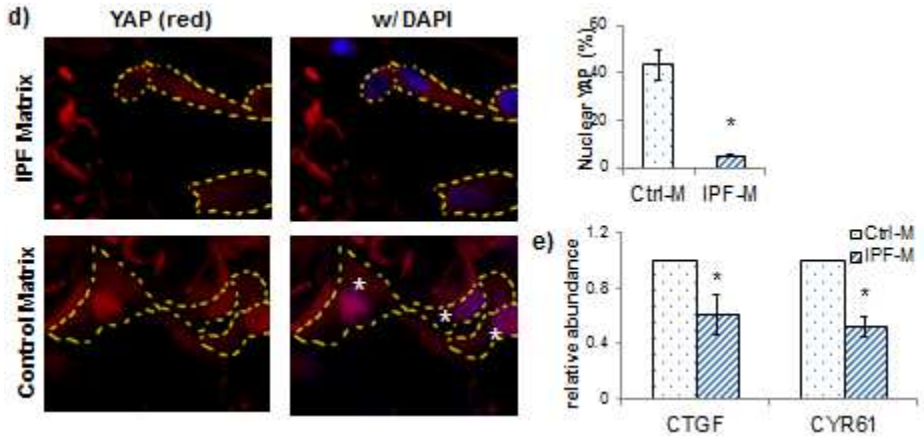

Figure B.7: YAP is suppressed by IPF-ECM. Lung fibroblasts were cultured on Ctrl- or IPF-ECM for 24 hours. a) Shown is an immunoblot of YAP expression normalized to GAPDH (representative blot), 3 independent experiments using 3 lung fibroblast lines designated L1, L2, and L3). Summary densitometry is shown in the right panel. b) mRNA abundance of YAP normalized to GAPDH (n=3 independent replicates). c) Lung fibroblasts were pre-incubated with 5uM MG132 for 4 hours and then cultured on Ctrl- or IPF-ECM for 4 or 8 hours. Immunoblot for YAP and GAPDH shown, and densitometry is shown on right panel. d) YAP Immunofluorescence (images are representative of 2 independent replicates; summary quantification shown in right panel). e) qPCR of CTGF and CYR61 normalized to GAPDH (n = 3 independent replicates).

Prior studies of YAP expression in IPF indicate that YAP abundance is low in IPF lung fibroblasts as compared to control lung fibroblast counterparts [Liu 2014], and histological analysis of YAP expression did not report specifically in fibroblastic foci, the signature diagnostic lesion in IPF. We therefore performed histological analysis of YAP expression in IPF lung tissue samples (specimens from 3 patients) with special attention to expression in fibroblastic foci. In order to identify active IPF fibroblastic foci, we immunostained for anti-human procollagen type I (**Figure B.8a**). Serial sections were immunostained for YAP (**Figure B.8b**).

The analysis revealed that cells in fibroblastic foci manifesting active type I collagen synthesis displayed low YAP expression as compared to surrounding tissue. These data are in accord with the diffuse YAP staining pattern previously reported in IPF [Liu 2015].

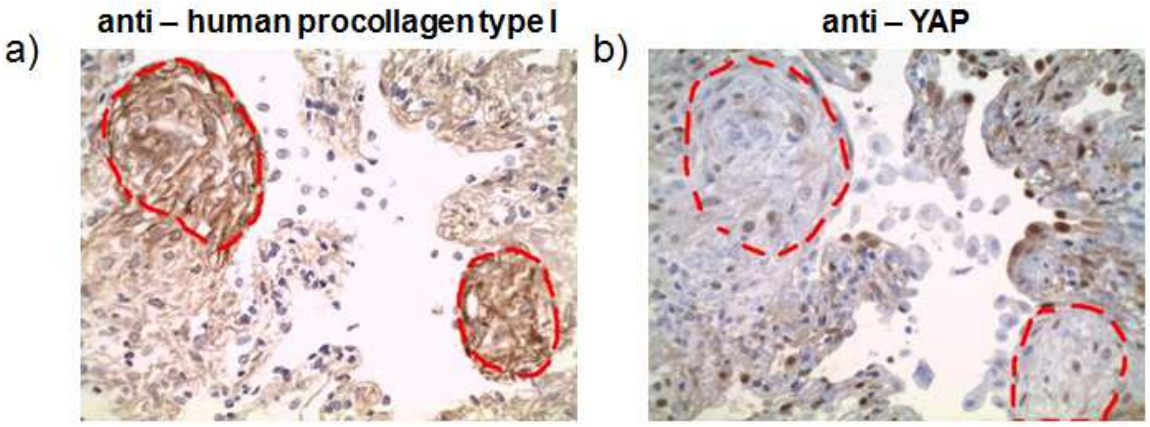

Figure B.8: Fibroblastic foci are low in YAP expression. Histological stains were performed on serial sections of IPF tissue. a) Active fibroblastic foci were identified by immunostain for type I collagen, b) and immunostain for YAP. (n = 3 IPF patients, representative image shown)

To further explore the issue of stiffness, we examined YAP expression on soft and stiff PA gels coated with type I collagen. In accord with prior studies using mesenchymal stromal cells [Dupont 2011] and lung fibroblasts [Liu 2015], lung fibroblast Yap abundance was unchanged on stiff gels (**Figure B.9a**), YAP subcellular localization was predominantly nuclear on stiff gels (**Figure B.9b**), and YAP target genes were upregulated on stiff gels (**Figure B.9c**). These results exclude stiffness *per se* as the primary driver of the YAP-miR-29 axis

pathology on IPF-ECM, and point to a more complex set of influences that may include interactions among mechanical properties, composition, and topography.

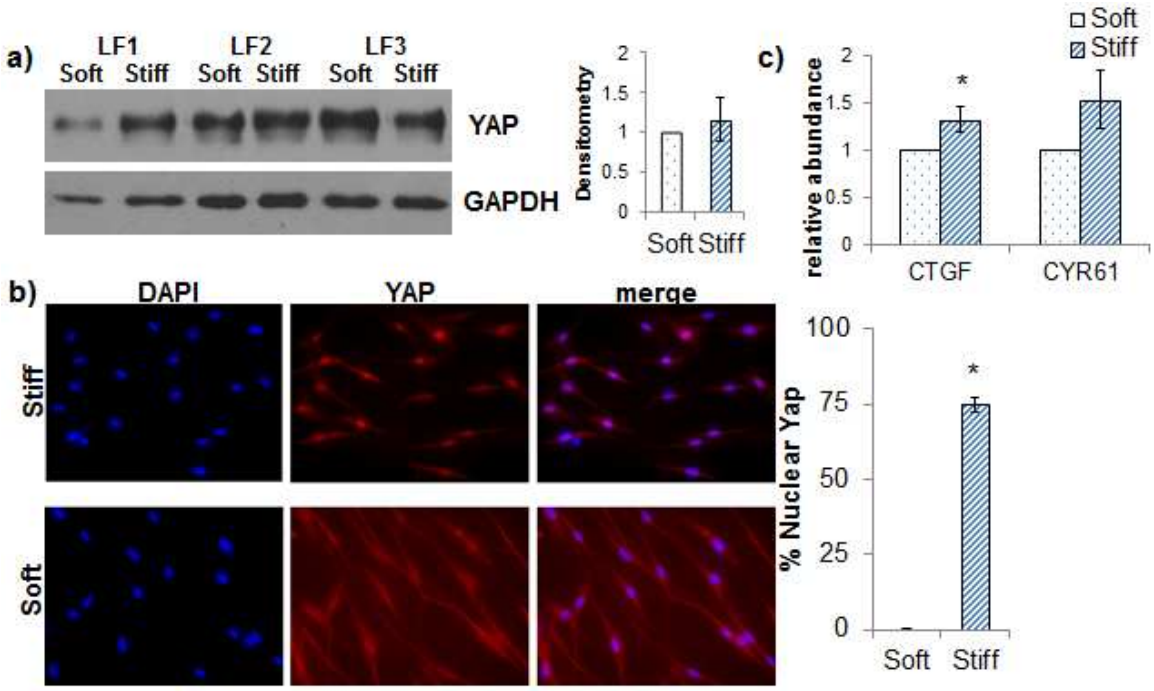

Figure B.9: Stiffness drives YAP activation. Primary lung fibroblasts were cultured on soft or stiff PA gels for 24 hours. a) Immunoblots for YAP and GAPDH (n = 3 independent replicates, densitometry on right panel). b) Immunofluorescence of anti-YAP on soft or stiff PA gels (n = 3 independent replicates, quantification on right panel). c) qPCR of CTGF and CYR61 normalized to GAPDH (n = 3 independent replicates).

B.3.4 YAP restoration does not rescue microRNA-29 by IPF-ECM

Currently, our data show YAP expression coincides with miR-29 expression; IPF-ECM drives low YAP and low mature miR-29 expression and stiff PA gels drives nuclear/active YAP and high mature miR-29 expression. To determine whether restoring YAP levels in fibroblasts rescues miR-29 expression

on IPF-ECM, we transduced lung fibroblasts with constructs encoding stably active YAP mutants resistant to proteosomal degradation (YAP S127/381A {FLAG tagged}) and a constitutive active YAP (5SA – S61/109/127/164/381A {Myc tagged}) [Zhao 2010]. Immunoblot shows ectopic expression of YAP mutants in fibroblasts (**Figure B.10a)**. As a functional readout of YAP expression, we found that transcriptional targets of YAP (CTGF and CYR61) are transcriptionally up-regulated in fibroblasts cultured on either Ctrl- or IPF-ECM (**Figure B.10b & d**). YAP S127/381A increased both transcript levels above controls, and constitutive active YAP 5SA increased transcript levels at higher levels than control and YAP S127/381A on both ECM's. In accord with Tumaneng et al., YAP transcriptionally activates precursor microRNA-29b-1/a in fibroblasts cultured on either Ctrl- or IPF-ECM (**Figure B.10c &e**). MiR-29b-2/c is under a different regulatory promoter [Mott 2010] and not up-regulated by YAP in our system. Although miR-29a precursor is up-regulated by mutant YAP's, mature miR-29a levels do not change in YAP expressing fibroblasts on either ECM (**Figure B.10f**). IPF-ECM tightly regulates low baseline levels of mature miR-29, and YAP restoration in fibroblasts cultured on Ctrl-ECM suppresses miR-29 to baseline IPF-ECM levels. Constitutive active YAP expression has been shown to suppress global microRNA processing by sequestering an essential microRNA processing machinery (DEAD-box RNA helicase – p72) [Mori 2014]. Active YAP does not further suppress mature miR-29 levels as

compared to vector treated fibroblasts on IPF-ECM, thus suggesting that microRNA processing is deregulated by IPF-ECM.

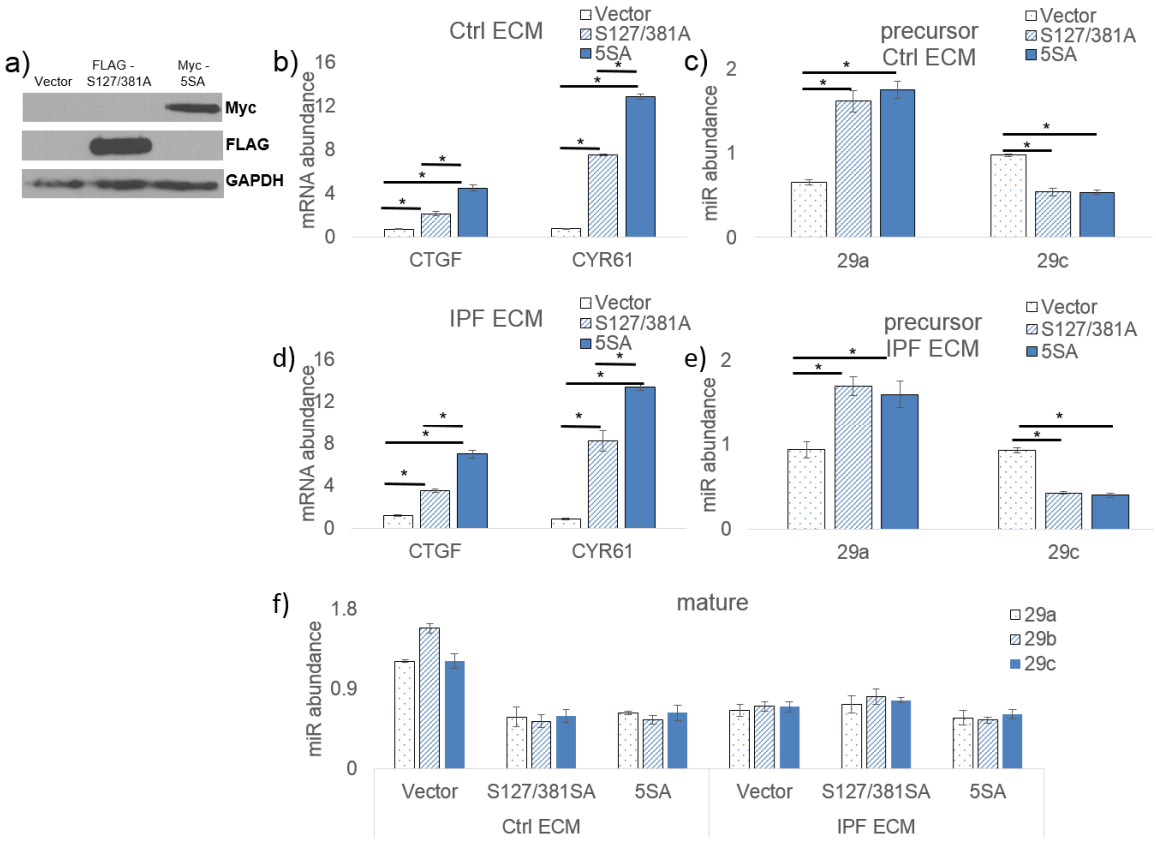

Figure B.10. YAP does not restore mature microRNA-29 expression. a) Lung fibroblasts were transduced with vector, YAP S127/381A – FLAG, or YAP 5SA – MYC for 48 hours and ectopic YAP expression is shown by immunoblot for FLAG, Myc, and GAPDH expression. b & d) Transduced lung fibroblasts were cultured on Ctrl- or IPF-ECM for 18 hours and qPCR for CTGF and CYR61 expression was normalized to GAPDH, c & e) precursor miR-29a and -29c expression was normalized to GAPDH, and f) mature miR-29a, -29b, and -29c was normalized to RNU6 (n = 2, representative experiment shown)

We also determined whether YAP suppression would decrease miR-29 expression by Ctrl-ECM. YAP suppression was determined by immunoblot (**Figure B.11a**), and YAP downstream transcriptional targets (CTGF and CYR61) served as a readout for YAP suppression (**Figure B.11b**). However YAP suppression was insufficient to suppress precursor or mature miR-29a and -29c expression when cultured on Ctrl-ECM (**Figure B.11c & d**). Collectively, these data suggest that YAP does not mediate miR-29 regulation by ECM.

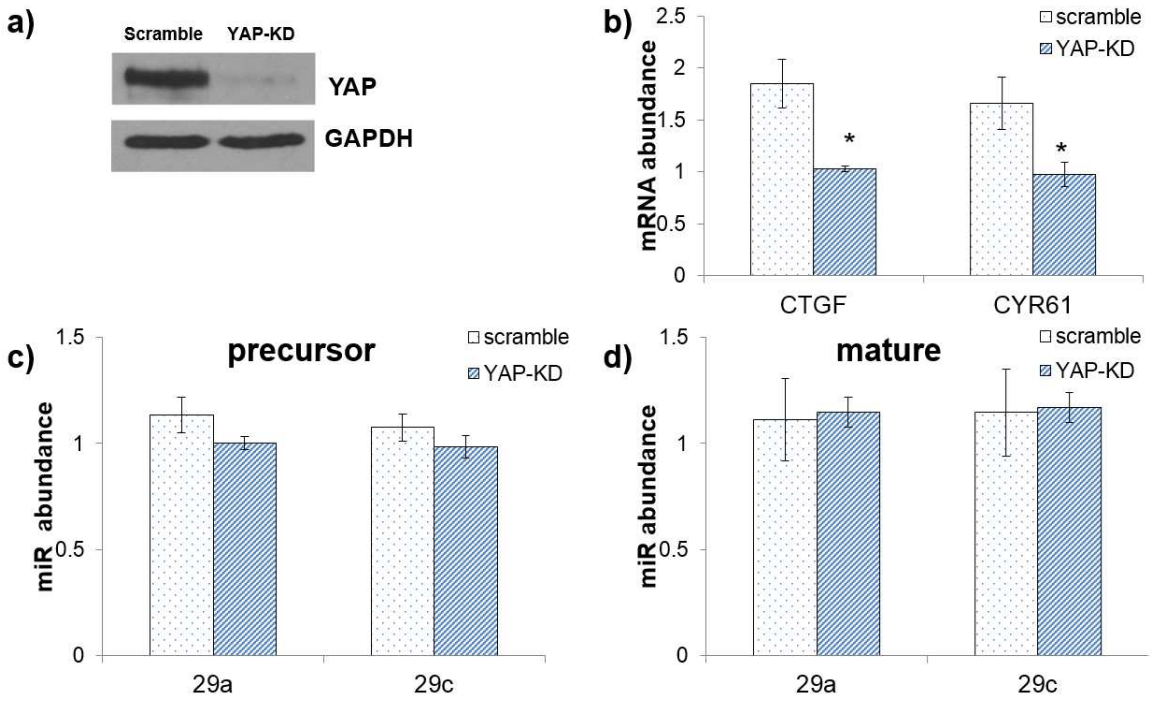

Figure B.11: YAP suppression does not suppress miR-29 expression. YAP was stably knocked down in primary lung fibroblast using shRNA with a pGIPZ lentivirus delivery system for 72 hours, and then cultured on Ctrl-ECM for 18 hours. a) Immunoblot for YAP and GAPDH. b) qPCR of CTGF and CYR61 normalized to GAPDH. c) Precursor miR-29a and -29c qPCR

normalized to GAPDH. d) Mature miR-29a and -29c qPCR normalized to RNU6. (n = 3, representative experiment shown)

B.3.5. IPF-ECM suppresses microRNA-29 processing post-microprocessor complex

Primary microRNA's are processed into precursor microRNA by the microprocessor complex (Drosha/DGCR8) by cleaving the microRNA Stem Loop. To determine whether microRNA processing is altered by ECM or stiffness, we measured microRNA processing activity. MicroRNA processing activity is a luciferase based assay where Firefly luciferase has a microRNA Stem Loop (recognized by the microprocessor complex) encoded into the 3'UTR [Mori 2014]. MicroRNA processing/cleavage of the Stem Loop destabilizes luciferase mRNA and a decrease of luciferase activity is measured as microRNA processing activity. Interestingly, microRNA processing activity is increased by both IPF-ECM and stiffness (**Figure B.12a & b**). To determine if microprocessing is altered specifically for miR-29, we quantitated primary miR-29a and precursor miR-29a (precursor assays quantitate both Pri-miR and Pre-miR) to indirectly quantitate precursor miR-29a abundance (**Figure B.12c & d**). Relative precursor miR-29a abundance is unchanged by ECM. Collectively, this suggests that microprocessor complex (Drosha, DGCR8) is functional on IPF-ECM, and that microRNA processing deregulation occurs at the level of post-microprocessor complex.

To determine whether IPF-ECM blocks microRNA processing on a larger scale as compared to Ctrl-ECM, we sought to quantify a panel of mature microRNA's (microRNA 96, 192, 21, 29a, 29b, and 29c). Using 3 – independent replicates, we found that IPF-ECM suppresses mature microRNA levels (**Figure B.12e**). We also sought to determine whether microRNA processing is deregulated by stiffness (**Figure B.12f**). Our data indicate that microRNA processing is suppressed by IPF-ECM, and that stiffness alone up-regulates microRNA processing. This suggests that deregulation must be on a global scale and not specific to miR-29 alone.

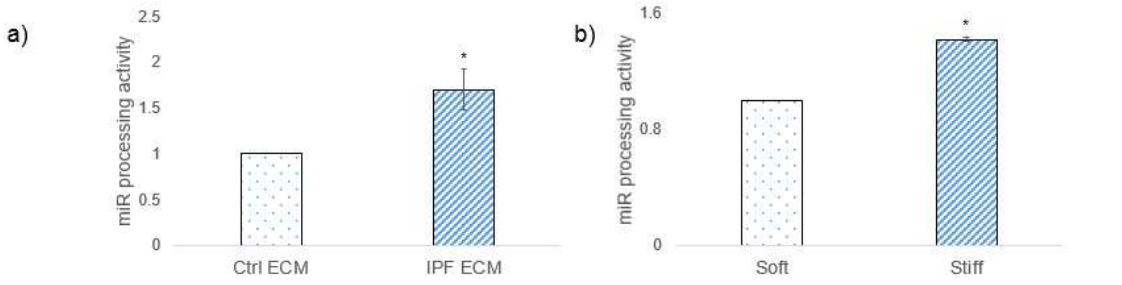

d)

miR-29a	Relative Precursor	Std. Dev.
Ctrl-ECM	40%	+/-5%
IPF-ECM	44%	+/-4%

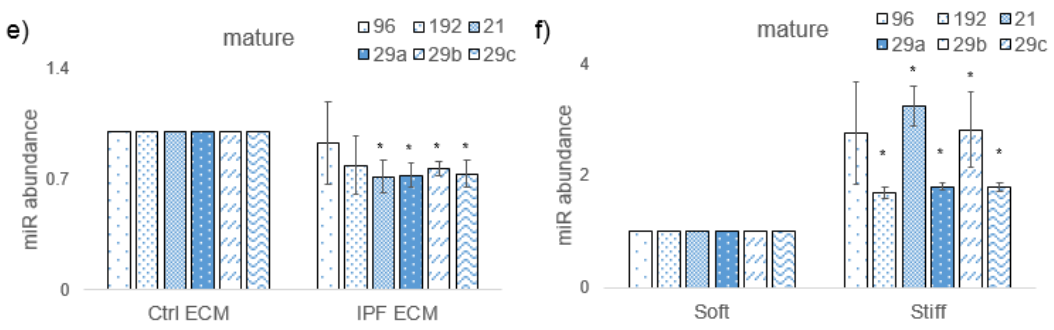

Figure B.12. IPF-ECM regulates microRNA processing post microRNA processing complex. a & b) MiR processing activity (plotted as inverse of luciferase activity) in primary lung fibroblasts cultured on Ctrl- or IPF-ECM and Soft or Stiff PA gels for 24 hours (n = 3 independent replicates or n = 2 independent replicates, respectively). **c)** Primers were designed for miR-29a Stem Loop and primary miR. Precursor miR can be determined by the difference of Stem Loop and Primary miR. **d)** Relative precursor abundance (n = 1). **e & f)** Panel of mature microRNA expression of primary lung fibroblasts cultured on Ctrl- or IPF-ECM and Soft or Stiff PA gels (n = 3 independent replicates for both).

B.4 Discussion

Our results demonstrate that pathological ECM plays a role in disease progression. Although the mechanical property of stiffness has been shown to drive fibrotic features in fibroblasts [Huang 2012, Liu 2014], our data show that primary lung fibroblasts cultured on synthetic polyacrylamide hydrogels simulating IPF stiffness up-regulates mature miR-29 expression (**Figure B.6 and B.12**). In accord with IPF pathology, authentic decellularized IPF lung tissue (IPF-ECM) suppresses mature miR-29 in primary lung fibroblasts (**Figure B.3, B.6, and B.12**). Our group has previously shown that miR-29c was suppressed by IPF-ECM and this translationally activates ECM genes at the polyribosome

recruitment level [Parker 2014]. This suggests that stiffness alone many not be the primary driver of miR-29 expression. Not only is IPF-ECM stiffer than its control counterparts, but both its composition and topology are altered [Booth 2012]. ECM components, such as Fibronectin-EDA, has been shown to drive myofibroblast differentiation of primary fibroblasts [Bhattacharyya 2014], and culturing primary fibroblasts on 3-dimensional grooves simulating topological alterations has been shown to regulate collagen deposition and matrix-metalloproteinase expression [Brydone 2011]. Our study highlights the use of authentic ECM as a model of human disease versus using single parameters of ECM properties.

Cells interact with their environment through multiple cell surface proteins such as integrins to exert internal cellular signals. Mechanical signals, such as stiffness, cell polarity, and adhesions have been shown to be mediated through Hippo pathways effector protein YAP [Dupont 2011, Moroishi 2015]. YAP has been shown to activate primary lung fibroblasts in a stiffness-dependent manner [Liu 2014]. We show that mutant YAP physiological up-regulation of miR-29b-1/a transcription does not restore mature miR-29 expression by IPF-ECM (**Figure B.10 and B.11**), indicating that YAP is not responsible for miR-29 deregulation in IPF. These studies, however, suggest a more complex role for microRNA processing deregulation by IPF-ECM.

Global microRNA processing suppression is a theme in cancer and IPF [Mori 2014, Oak 2011], and our data show that miR-29 processing is suppressed

by IPF-ECM (**Figure B.6 and B.10**). We show that microRNA processing activity is increased by IPF-ECM and that primary miR-29a is similarly processed to precursor miR-29a by either ECM which suggests that microRNA processing is deregulated at the level of post-microprocessor complex (**Figure B.12**). Therefore, IPF-ECM suppresses microRNA processing at the level of nuclear export, or cytoplasmic microRNA processing regulation (**Figure B.13**). Unbound precursor microRNA is rapidly degraded in the cytoplasm unless it is bound to Dicer or Argonaute proteins. Deregulation of Dicer or Argonaute proteins causes global suppression of mature microRNA processing [Ha 2014]. Oak et al. showed that 36 of 88 investigated mature microRNA's are suppressed in IPF *ex vivo*. They show that the expression of Dicer1, Ago1, and Ago2 are suppressed in rapid progressive IPF fibroblasts and that levels of Ago1 and Ago2 in IPF patient lung biopsies are deregulated [Oak 2011]. This supports a role of microRNA processing defects at the level of cytoplasmic microRNA processing in our decellularized ECM model. Further studies looking at ECM-mediated effects on Dicer and Argonaute are warranted.

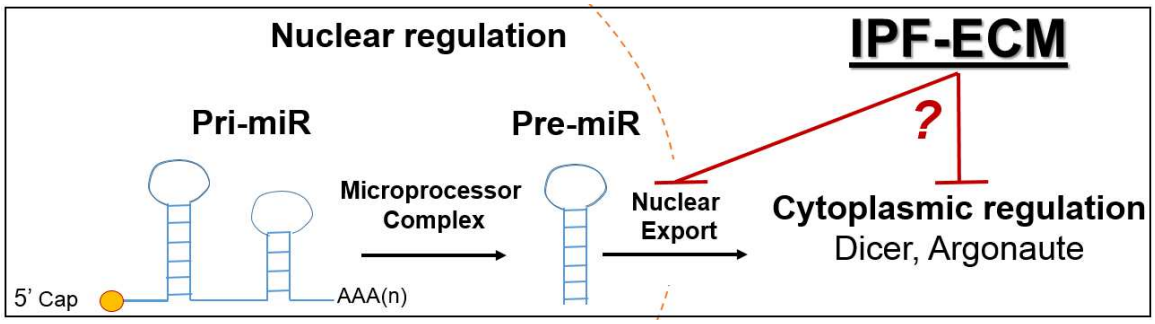

Figure B.13. Model: IPF-ECM deregulates microRNA-29 processing at the level of post-microprocessor complex

B.5 Conclusion

IPF is a terminal disease with few therapeutic treatment options. We sought to understand disease progression by culturing primary human lung fibroblasts on decellularized IPF tissue in an effort to understand how pathological ECM modulates miR-29 expression (a key fibrotic regulator). We find that IPF-ECM deregulates miR-29 processing, and that this is not a stiffness mediated affect. Further studies addressing how IPF-ECM deregulates key microRNA processing machinery will help us unravel pathological pathways in IPF progression.

Chapter C. Published collaborative studies providing insights into translational control of IPF and cancer

As part of my training, I was involved with a collaborative network that included joint laboratory meetings and I joint experiments with the Henke (IPF expert) and Polunovsky (translational control expert) laboratories. These activities led to a series of co-authored publications within the field of translational control of IPF and breast cancer. I will summarize each publication below and highlight my involvement that merited co-authorship.

C.1. Alexey O. Benyumov, Polla Hergert, Jeremy Herrera, Mark Peterson, Craig Henke, & Peter B. Bitterman (2012) A novel zebrafish embryo

xenotransplantation model to study primary human fibroblast motility in health and disease. *Zebrafish*. 9(1):38-43

In an effort to establish a cost-effective and efficient *in vivo* model of IPF, Alexey Benyumov set out to determine the intrinsic motility of primary lung fibroblasts when transplanted into zebrafish embryos. In this assay, ~100 fibroblasts are microinjected into a developing zebrafish embryo and allowed to develop for 48 hours. Our studies show that IPF lung fibroblasts have increased motility in zebrafish embryos as compared to control lung fibroblasts [Benyumov 2012]. This shows that IPF fibroblasts have the intrinsic capacity to migrate *in vivo*.

My effort in this project was to determine fibroblast viability after zebrafish embryo transplantation by histological analysis. In order to determine viability, I immunostained for anti- human Ki67 (proliferation marker). We were able to show that fibroblasts are viable within zebrafish embryos after 48 hours of transplantation [**Figure C.1**]. This collaboration was fruitful as it gave me expertise in handling and sectioning 2-3 mm developing zebrafish.

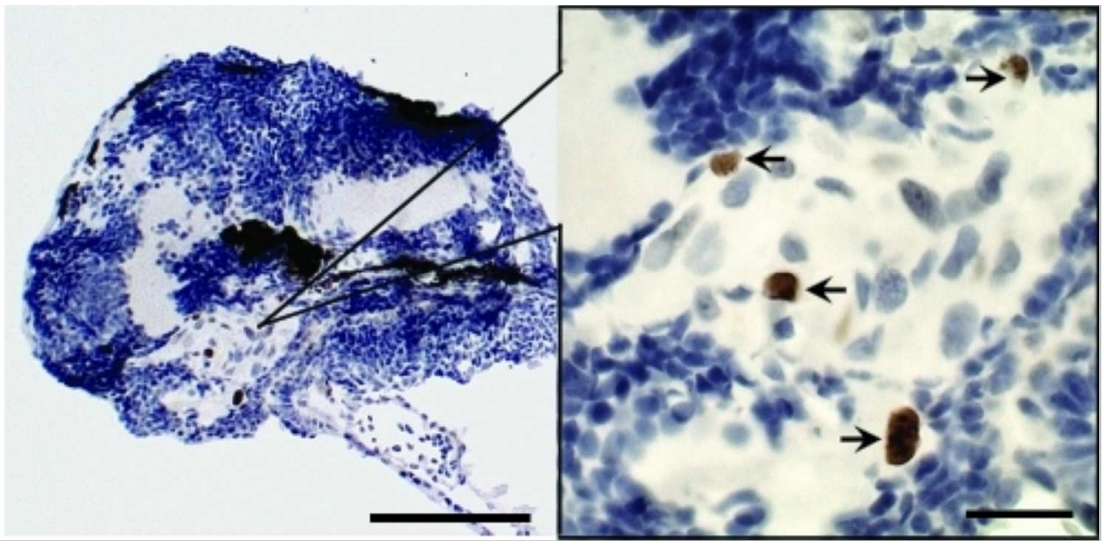

Figure C.1: Fibroblast survive in zebrafish xenografts. Image of sagittal section of an embryo immunostained with anti - human Ki67. *Arrow* points to the graft area in the head region of the embryo. *Inset:* Ki67+ cell nuclei in the graft body. *Arrows* point to the labeled nuclei of the engrafted cells. Scale bars: 100 μm in C.1. and 30 μm in C.1. inset.

C.2. Hong Xia, Vidya Bodempudi, Alexey Benyumov, Polla Hergert, Damian Tank, Jeremy Herrera, Jeff Braziunas, Ola Larsson, Matthew Parker, Daniel Rossi, Karen Smith, Mark Peterson, Andrew Limper, Jose Jessurun, John Connett, David Ingbar, Sem Phan, Peter B. Bitterman, & Craig A. Henke (2014) Identification of a cell-of-origin for fibroblasts comprising the fibrotic reticulum in Idiopathic Pulmonary Fibrosis. *Am J Pathol*. 184(5):1369-1383

In order to treat IPF, it is important to understand the source of lung myofibroblasts. The source of myofibroblasts has been intensively studied and data suggest a variety of origins from the differentiation of resident fibroblasts, to circulating bone marrow-derived progenitor cells, through epithelial to

mesenchymal transition (EMT) [Rosas 2015]. In this study, we sought to isolate mesenchymal progenitor cells from control and IPF lungs by sorting for progenitor marker stage-specific embryonic antigen 4 (SSEA4), and determine whether their progeny retain IPF hallmark characteristics. We show that IPF mesenchymal progenitor cell progeny had an increased Akt signaling axis, increased expression of alpha-smooth muscle actin and type I collagen, and form a fibrotic reticulum in zebrafish and mouse models demonstrating that fibrogenic mesenchymal progenitors are a cell-of-origin in IPF [Xia 2014].

My efforts in this project were to determine whether the IPF mesenchymal progenitor cell progeny formed fibrotic lesions in mouse and zebrafish models of IPF by histological analysis. Immunocompromised mice were tail vein injected with 1×10^6 progeny, and sacrificed after 60 days. Immunohistochemistry for anti-beta-2 microglobulin was performed to identify human-derived cells within the lungs of mice (immunocompromised mice lack beta-2 microglobulin). Only progeny cells derived from IPF mesenchymal progenitors formed both intravascular and perivascular fibrotic lesions in the lungs of mice, and these fibrotic lesions expressed collagen as seen by trichrome stains (**Figure C.2a**). Similarly, progeny cells derived from IPF mesenchymal progenitor cells formed grafts in developing zebrafish that expressed higher levels of human pro-collagen type I than control progeny cells (**Figure C.2b**).These experiments show that IPF mesenchymal progenitor cell progeny form fibrotic lesions *in vivo*, thus are a cell-of-origin in IPF.

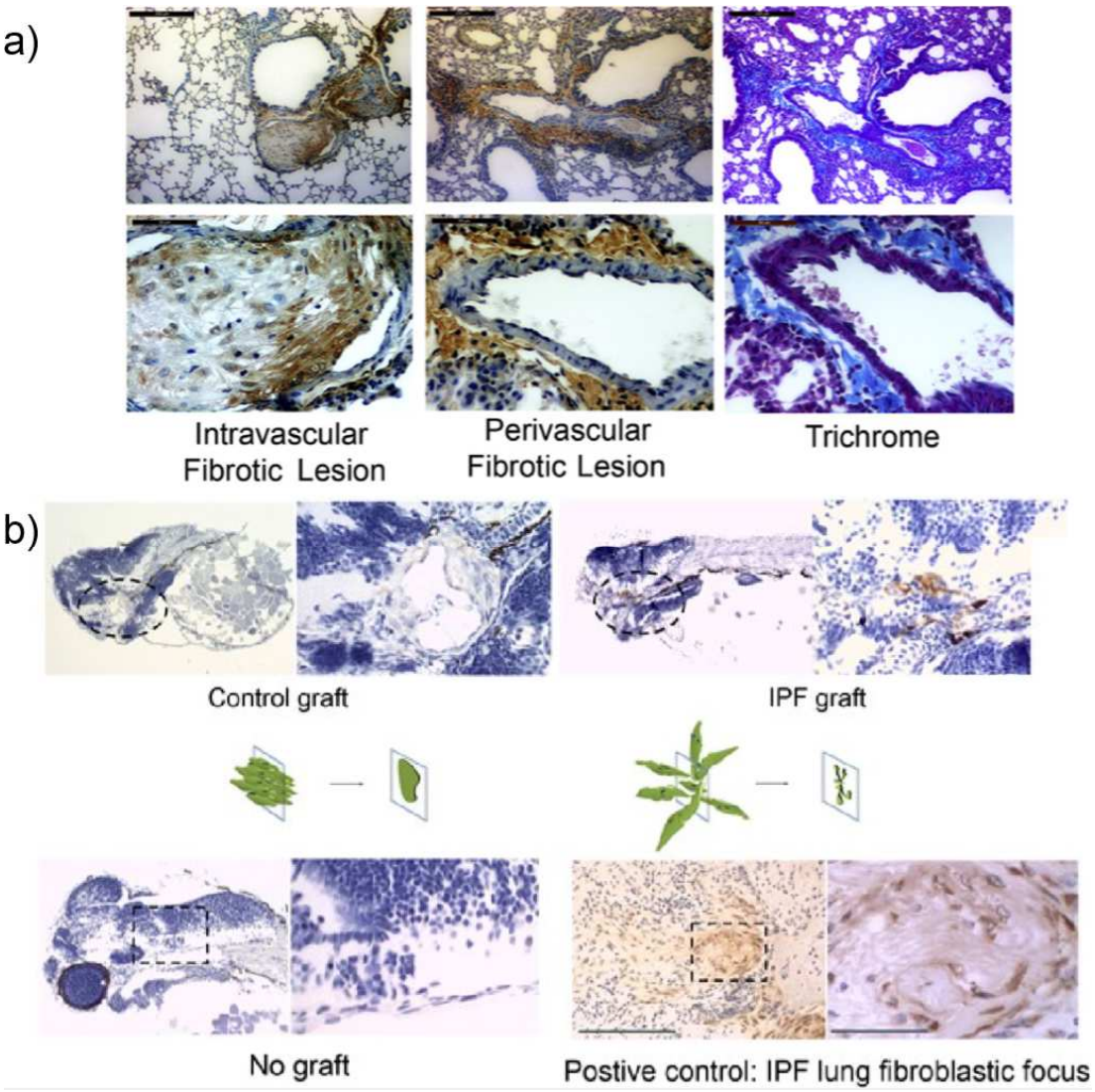

Figure C.2. IPF mesenchymal progenitor cells form fibrotic lesions *in vivo*. a) IPF mesenchymal progenitor cell progeny were tail vain injected into immunocompromised mice. Anti-β2 microglobulin immunostain was performed to identify human derived cells and intravascular and perivascular fibrotic lesions were identified (2 left panels). Trichrome stain was done to identify collagen expression on a serial slide (deep blue stain, right panel). b) Anti - human procollagen type I was immunostained in zebrafish bearing progeny grafts. Sham-treated embryos with no graft at 48 hours after transplantation served as a negative control (lower left panel). Human IPF lung tissue displaying procollagen type I immunoreactive cells in a fibroblastic focus served as a positive control for the procollagen type I staining procedure (lower right panel).

Immunoreactive cells were detected in the IPF graft-bearing embryos (upper right panel). Control graft-bearing embryos showed light immunoreactive cells. Scale bars: 50 μm.

C.3. Vidya Bodempudi, Polla Hergert, Karen Smith, Hong Xia, Jeremy Herrera, Mark Peterson, Wajahat Khalil, Judy Kahm, Peter B. Bitterman, & Craig A. Henke (2014) miR-210 promotes IPF fibroblast proliferation in response to hypoxia. *Am J Physiol Lung Cell Mol Physiol*. 307(4):L283-L294

As fibroblast accumulate in the lung airspaces where they actively synthesize and assemble ECM, patients suffocate due to the lack of oxygen exchange. The lack of oxygen in the lung produces a hypoxic environment which is associated with fibroblast growth [Bradley 1978]. Vidya Bodempudi hypothesized that hypoxia will drive IPF fibroblast proliferation and lung fibrosis. In this study, HIF-2α (hypoxia-inducible transcription factor 2) was shown to stimulate IPF fibroblast proliferation by up-regulating miR-210 which is a known target of genes that regulate cell proliferation and apoptosis [Qin 2014]. In this study, miR-210 suppressed MNT (c-myc inhibitor) in lung fibroblasts which results in increased fibroblast proliferation. Knockdown of HIF-2α suppressed miR-210, and reversed IPF fibroblast proliferation. This study highlighted miR-210 regulation by hypoxia as a mechanism for increased fibroproliferation in IPF [Bodempudi 2014].

My efforts in this study were to validate that hypoxic markers HIF-2α and carbonic anhydrase-IX were expressed in fibrotic foci within IPF tissue. IPF or control lung tissue (n = 3 each) was sectioned and immunostained for anti-HIF-

2α and anti-CA-IX. IPF foci (insets) stained positive for both CA-IX and HIF-2α, while control lung tissue showed no reactivity. This data shows that IPF fibrotic foci (pathological feature in IPF) are hypoxic.

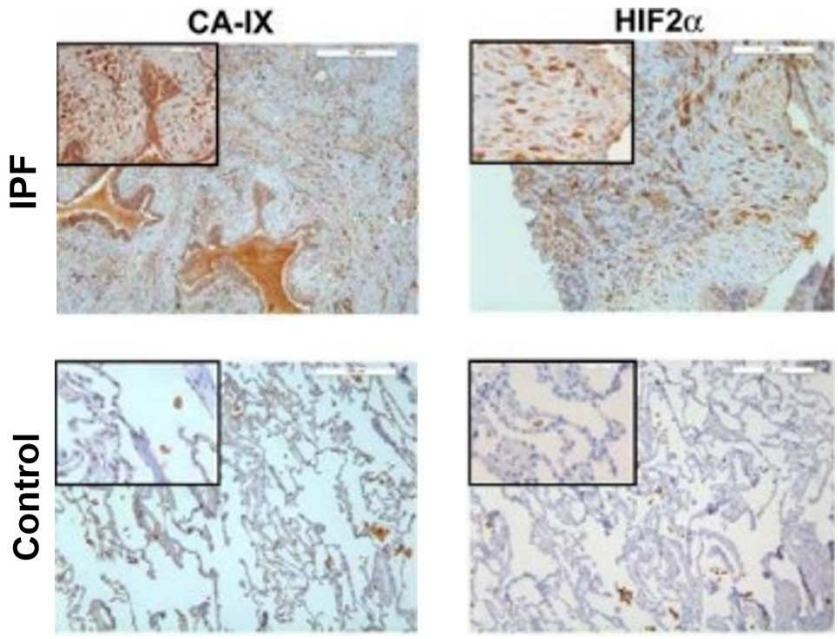

Figure C.3. IPF fibroblastic foci are hypoxic. IPF or control tissue was immunostained for CA-IX or HIF-2α. CA-IX (Left panels) was expressed in IPF foci (upper-inset) and absent in control lung tissue (lower). HIF-2α (right panels) was expressed in IPF foci (upper-inset) and absent in control lung tissue (lower).

C.4. Svetlana Avdulov, Jeremy Herrera, Karen Smith, Mark Peterson, Jose R. Gomz-Garcia, Thomas C. Beadnell, Kathryn L. Schwertfeger, Alexey O. Benyumov, Carlos Manivel, Shunan Li, Anja-Katrin Bielinsky, Douglas Yee, Peter B. Bitterman, & Vitaly A. Polunovsky (2015) eIF4E Threshold Levels

Differ in Governing Normal and Neoplastic Expansion of Mammary Stem and Luminal Progenitor Cells. *Cancer Research*. 75(4): 687-697

As a co-first author with Svetlana Avdulov from the Polunovsky laboratory, I began to define the mechanism by which eukaryotic initiation factor 4E (eIF4E) promotes breast cancer initiation. eIF4E is a proto-oncogene that drives primary cell transformation [Avdulov 2004] and tumor formation in animal models [Ruggero 2004]. eIF4E is the rate limiting step to protein translation initiation and binds the 5' cap of mRNAs while recruiting initiation factor eIF4G and eIF4A to form the translation preinitiation complex - eIF4F. Not all mRNAs are created equally, and studies show that when eIF4F is modulated, eIF4F amplifies major receptor signaling pathways [Bitterman 2012]. However, in order to form cancer, a wide range of anti-cancer defense mechanisms must be shut down. One mechanism is oncogene-induced stress where a strong oncogenic response causes cellular apoptosis (c-Myc) or senescence (hRasV12) [Murphy 2008 and Serrano 1997, respectively]. Herein, we show that overexpression of eIF4E during pregnancy in mice promotes self-renewal of mammary luminal progenitor cells and drives neoplastic breast lesions. Increased DNA damage corresponded with increased eIF4E expression in breast luminal cells, and complementary *in vitro* studies show that eIF4E rescues human mammary epithelial cells from oncogene-induced stress that is usually lethal.

As a co-first author, I played a major role in the development of this project. My efforts in this study were to characterize the *in vivo* transgenic mouse

model via histological analysis and the *in vitro* model via immunocytochemical analysis. Transgenic FVB/N mice were created to express exogenous eIF4E (HA tagged) under the whey-acidic promoter (WAP). WAP is driven by lactation hormones and is active in mammary breast tissue during late pregnancy and lactation, and turned off during weaning when lactation hormone expression is off. In order to determine whether exogenous eIF4E (HA tagged) was expressed, immunostains for anti-HA were performed over sequential gestation after 15 days of lactation (**Figure C.4a**). We found that entire ductal/alveolar units are positive (or negative) for exogenous eIF4E, and that positive unit frequency increases with increased gestation. We determined that HA expression was restricted to luminal cells by double labeling HA with luminal marker cytokeratin 8 (K8) (**Figure C.4b**). To determine if eIF4E overexpression caused a proliferative advantage, immunostains for anti-Ki67 were performed (**Figure C.4c**). To our surprise, we did not see a difference in Ki67 expression until gestation 6+. To further validate that increased eIF4E induced proliferation, we double labeled for luminal marker K8 and proliferation marker Ki67 in WAP-4E mice and found that HA positive cells have increased expression of Ki67 (**Figure C.4d**). These data show that exogenous eIF4E expression drives proliferation in luminal mammary epithelial cells *in vivo*.

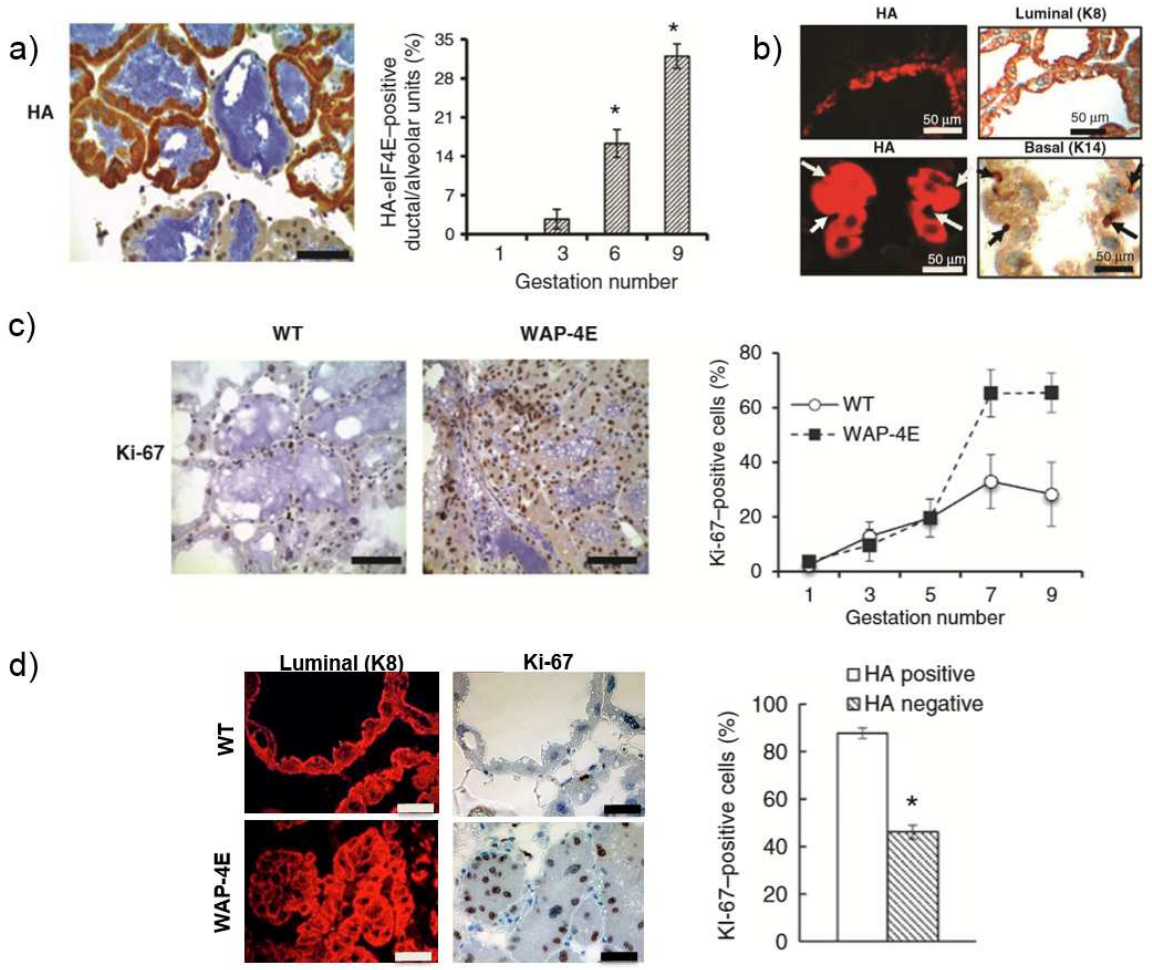

Figure C.4. Exogenous eIF4E-HA expression drives proliferation of luminal mammary epithelial cells *in vivo*. a) formalin-fixed paraffin-embedded sections of mammary glands (gestation 6, left panel) were immunostained for HA expression. HA-eIF4E positive mammary acinar/ductal structural units were quantitated (right panel, n=2). b) Fluorescent immunostain for HA (Cy3 – red) was overlapped with peroxidase immunostain for K8 (luminal marker) or K14 (basal marker). c) Representative image of mammary tissue from WT and WAP-4E females (gestation 9, day 15 of lactation) immunostained for Ki67 (left panel). Quantification during successive pregnancy/lactation cycles of WT and WAP-4E mice (right panel, n = 4). d) Immunostain for anti-HA (Cy3) overlapped with anti-Ki67 (brown) in WT and WAP-4E mice (left panel), and quantification (right panel, n = 5 mice per group).

To determine oncogenic effects of exogenous eIF4E expression in mammary tissue, we selected gestation 6 where increased Ki67 expression is observed, and performed carmine staining of complete mammary pads after 10 days of weaning which is necessary to see gross changes in mammary glands (**Figure C5a**). WAP-4E mice developed foci (#2) highlighted with yellow arrows, and closer analysis via H&E unmasked lesions (#3 and 4) in all WAP-4E mice. To determine whether these are hyperplastic lesions, we immunostained for Ki67 and performed TUNEL analysis to determine proliferation and apoptosis, respectively. After weaning, there is no difference in gross proliferation or apoptosis in mammary tissue after exogenous eIF4E expression is off (**Figure C.5b & e**). However, analysis of the lesions revealed increased proliferation and decreased apoptosis as compared to surrounding non-lesional tissue (**Figure C5.c-d & f-g**). To determine if these hyperplastic lesions persist, we show that lesions are present up to 45 days post-weaning (**Figure C.5h**). This data shows that exogenous eIF4E expression promotes tumor initiation that persists post-weaning.

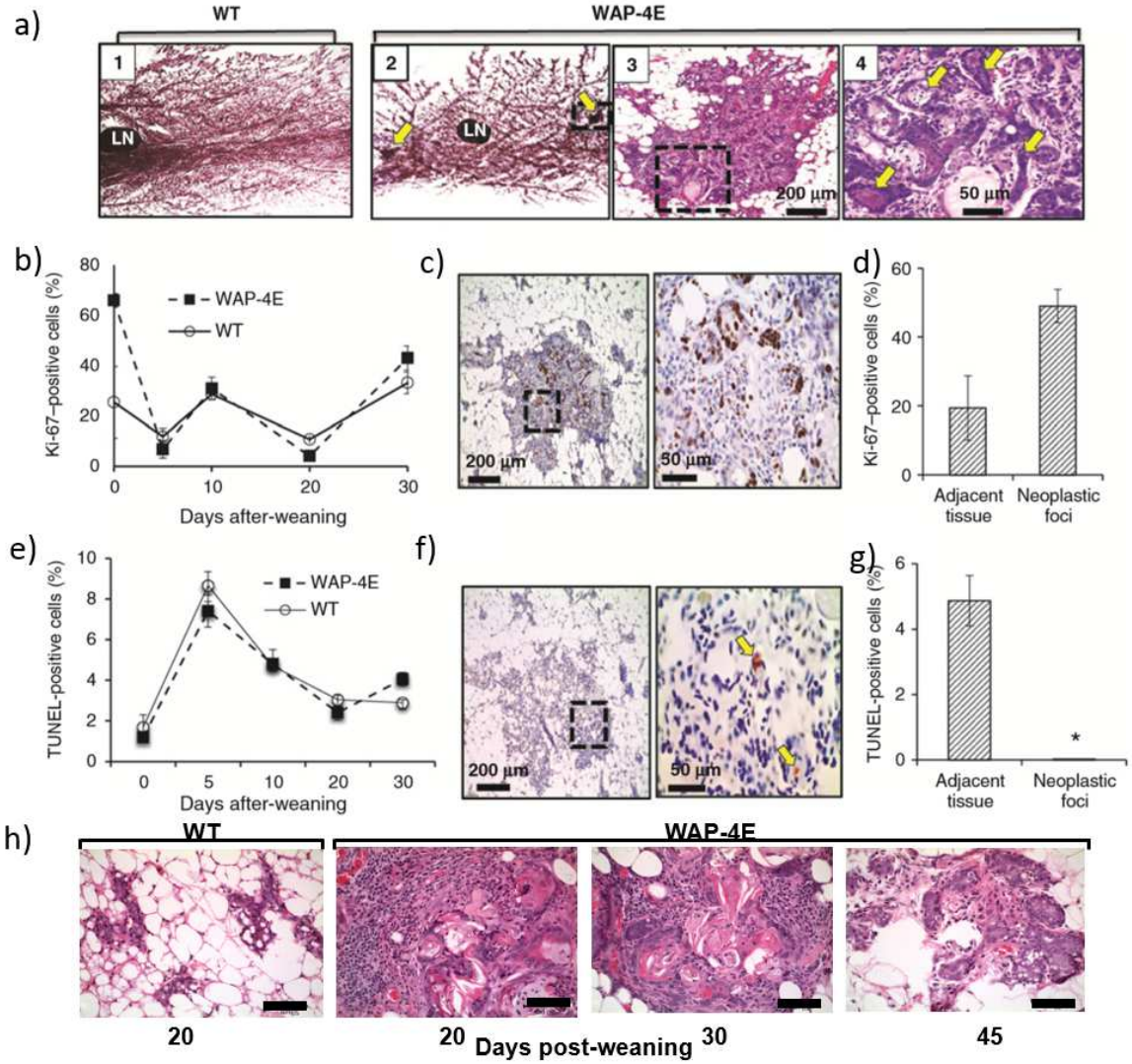

Figure C5: Exogenous eIF4E drives initiation of breast cancer that persists post-weaning. a) post-weaning whole mammary gland of multiparous WAP-4E females contain neoplastic foci of WT and WAP-4E females (gestation 9, day 10 post-weaning) were stained with carmine (1 and 2). Representative gland pictures and photo micrographs are presented (n=28). Arrows, neoplastic nodules; LN – lymph node. One nodule (shown in the boxed area, 2) was surgically removed, and 5-µm sections were stained with hematoxylin/eosin (3 and 4). Arrows, deformed acinar structures. b) Shown are the proliferative indices in post-weaning WT (n = 4) and WAP-4E (n = 4) mammary glands (gestation 8). C, representative image of the focus counterstained with hematoxylin and probed for expression of Ki-67 (brown). d) The relative numbers of Ki-67–

positive cells in neoplastic foci and in adjacent areas of mammary glands from WT (n = 3) and WAP-4E (n = 3). e) Time course of apoptotic activity quantified outside of neoplastic foci in post-weaning WT (n = 3) and WAP-4E mice (n = 3). f) Representative image shows scattered TUNEL-positive cells (arrows) in the WAP-4E neoplastic focus. g) Shown are the relative numbers of TUNEL-positive cells in neoplastic foci and in adjacent areas of post-weaning WAP-4E mammary glands (day 10 post-weaning; n = 3 mice). h) Hematoxylin and Eosin stain of WT and WAP-4E mice neoplastic foci over a range of days post-weaning.

FVB/N mice rarely present with spontaneous tumors. In our transgenic WAP-4E model in FVB/N mice, tumor formation was achieved. What we found was that WAP-4E drove luminal tumor formation (**Figure C.6**). This tumor was positive for K8 (luminal marker), and negative for basal markers (K5 and K14) and mesenchymal/myoepithelial markers (p63 and αSMA). This fits with our data where exogenous eIF4E is expressed in luminal epithelial cells.

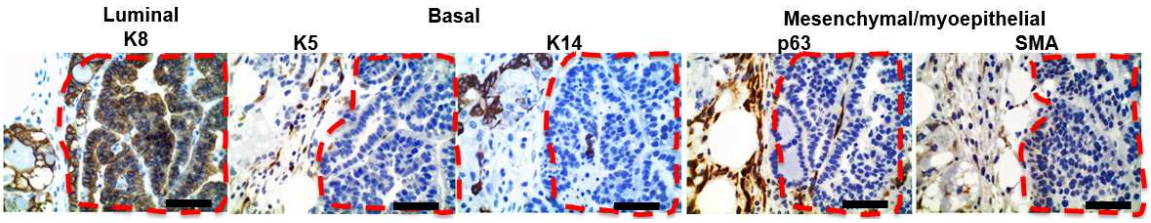

Figure C.6. WAP-4E drives luminal tumor formation. WAP-4E female tumor was sectioned and immunostained for anti-K8 (luminal marker), anti-K5 and anti-K14 (basal marker), and p63 and alpha-smooth muscle actin (mesenchymal/myoepithelial marker). Tumor area is enclosed with a red dotted line.

Early anti-cancer mechanisms exist to prevent cellular transformation. Oncogene mediated proliferation causes double-stranded breaks (DSBs) in DNA that signals a DNA-damage response (DDR) leading to cellular senescence and apoptosis. Single-stranded DNA (ssDNA) recruit replication protein A (RPA) to protect vulnerable ssDNA and orchestrates a phosphorylation cascade to phosphorylate the downstream effector H2AX (active form - γH2AX) [Zeman 2014]. To determine whether exogenous eIF4E causes a DDR, we measured expression of γH2AX in mammary epithelial cells *in vivo* (**Figure C7a**). WAP-4E animals have an increased number of γH2AX foci in luminal cells as compared to WT mice, whereas non-luminal cells are unaffected. To complement this data, we switched to a relevant *in vitro* system to determine whether eIF4E expression can overcome oncogene-induced apoptosis caused by hRasV12. Over expression of hRasV12 induces apoptosis in mammary epithelial cells, but co-expression of eIF4E rescues colony formation upon hRasV12 induction (data not shown). Co-expression of RPA and γH2AX in cells suggests broken DNA that leads to cell death, however if rescued by homologous recombination or repaired by other mechanisms, RPA is displaced and γH2AX is expressed alone. We show that eIF4E expression increases γH2AX expression alone which may explain rescue of oncogene induced apoptosis (**Figure C7b & c**). Together, these data suggest that eIF4E rescues cells from oncogene-induced stress and allows cellular transformation.

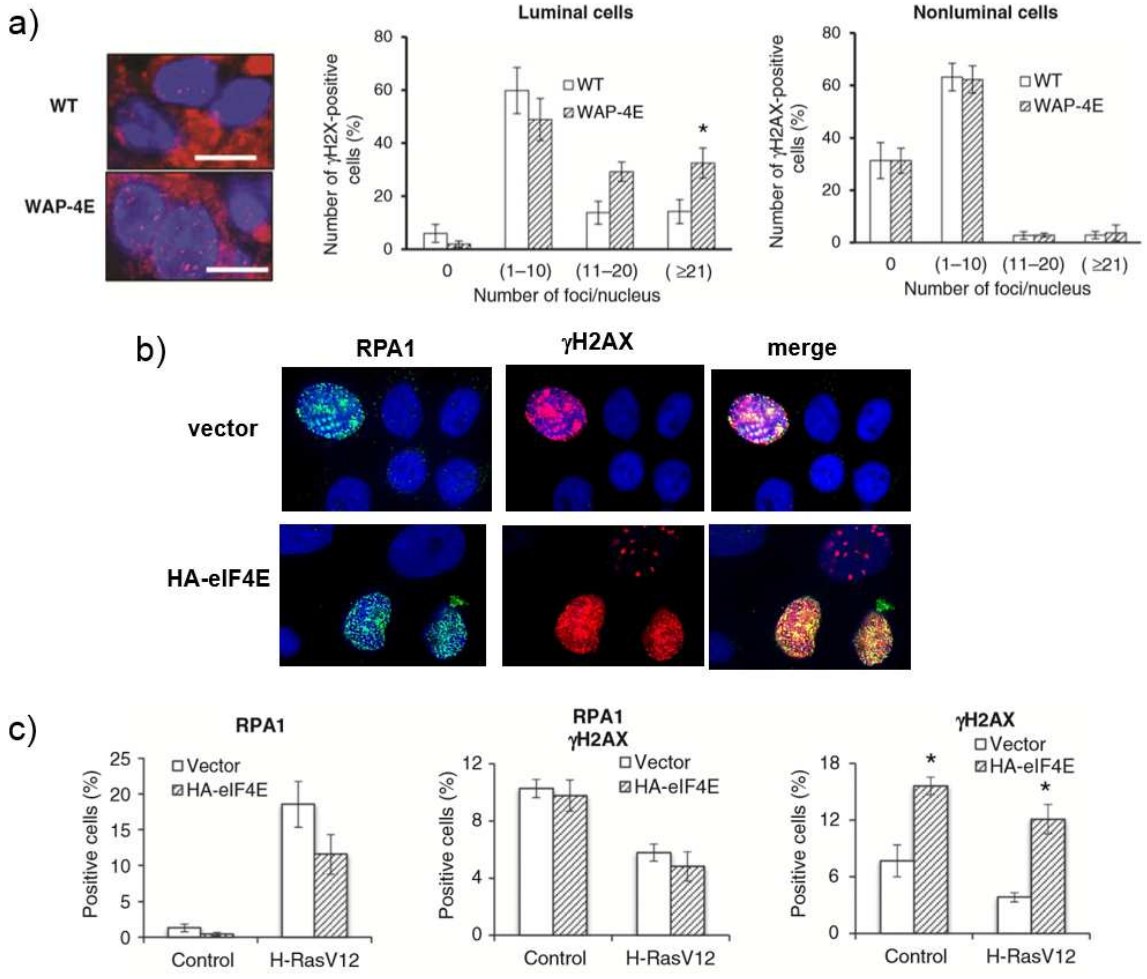

Figure C.7. Overexpressed eIF4E stimulates a replication stress response. a) Representative image of mammary epithelial cells from WT (n = 5) and transgenic (n = 5) mammary glands (left panel) immunostained with anti-γH2AX. Quantification of luminal cells (center panel) were performed by scoring number of foci per nucleus and the same was done for non-luminal cells (right panel). b) Representative image of anti-RPA and anti-γH2AX fluorescent stain of HMEC/hTERT cells with or without ectopic HA-eIF4E expression. c) Quantification of HMEC/hTERT or HMEC/hTERT/H-RasV12 transduced with HA-eIF4E immunostained for anti-RPA1 or anti- γH2AX. RPA positive alone (left panel), both RPA1/ γH2AX positive (center panel), or γH2AX positive alone (right panel). (n = 2)

To summarize the findings of this manuscript, we show that overexpression of eIF4E over the physiological maximum promotes the propagation of luminal progenitor cells (data not shown – mammosphere assay) that leads to the development of premalignant and malignant mammary lesions. We show that eIF4E induces DDR in mammary tissue, and that eIF4E expression induces pro-survival DDR during oncogene-induced challenges *in vitro*. This supports a model in which eIF4E causes continued hyperproliferation leading to genomic instability which can accumulate oncogenic mutations. eIF4E can rescue otherwise lethal oncogenic lesions to promote cellular transformation and tumor formation. (**Figure C.8**) [Avdulov 2014].

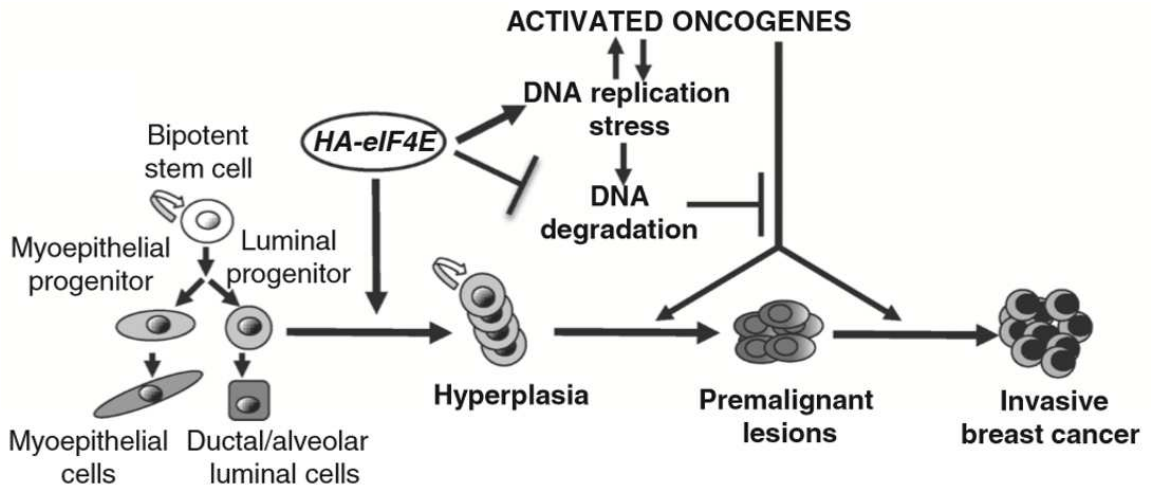

Figure C.8. Model of eIF4E-driven development of Pregnancy-associated Breast Cancer in transgenic mice.

C.5. Conclusions

My successful collaboration with Craig Henke and Vitaly Polunovsky has resulted in 1 first co-authorship and 4 co-authorships during the duration of my PhD training. These experiences strengthen my expertise in modeling IPF in animal models, and the understanding of molecular pathway deregulation in both IPF and cancer.

Chapter D. The Big Picture

As I reflect upon the scientific discoveries achieved during my PhD training, it is easy to get lost in the fine details and forget the big picture. Cells have the ability to sense their environment, and through sensing, modulate their cellular dynamics and functions that are measurable through experimental detection in the laboratory. We have created a new model to study IPF, and we asked a simple question: How do normal cells respond to decellularized human IPF tissue? We cultured normal fibroblasts (cell of interest in fibrosis) on authentic decellularized lung tissue from IPF patients, and measured relevant disease pathways. Herein we find that a diseased microenvironment causes a normal fibroblast to become fibrotic-like. Specifically, our data is the first to identify corruption of microRNA processing by the IPF fibrotic matrix itself as one mechanism for sustained connective tissue production in IPF.

The major clinical follow up question to this work is this: what is the cell/ECM interaction leading to microRNA processing deregulation in IPF? If we can unravel the ECM component(s) and/or the cell surface receptor(s)

responsible for this deregulation, pharmaceutical intervention against ECM/cell interfaces could block IPF progression. This is the overarching goal of our research, but we are still a long ways from unraveling this mystery.

Inside – Out and Outside – In signaling is mediated by integrins. Integrins are a heterodimeric protein composed of an α-subunit and β-subunit. There are 18 α-subunits and 8 β-subunits that can assemble into 24 distinct combinations. Integrin sense the extracellular environment and can send downstream signals to 232 genes to produce a cellular response [Winograd-Katz 2014]. Due to high complexity of IPF matrix, multiple integrin interactions in concert, and hundreds of downstream integrin effector targets in cells, it would be incredibly difficult to pinpoint which receptor and pathway is responsible for microRNA processing deregulation. With such complexities in understanding biological processes, tools have been created to begin uncoupling molecular pathways at global levels. Tools such as gene expression profiles, bioinformatics, and proteomics are helping us move forward into a new era of scientific discovery. Although this is out of the scope of my dissertation, this project will be followed up by the next graduate student and/or academic postdoctoral researcher. With that said, my adventure will continue in pursuit of scientific discoveries in understanding molecular pathways deregulated in disease.

References:

Benyumov, Alexey O, Polla Hergert, Jeremy Herrera, Mark Peterson, Craig Henke, and Peter B Bitterman (2012) A Novel Zebrafish Embryo Xenotransplantation Model to Study Primary Human Fibroblast Motility in Health and Disease. *Zebrafish.* 9(1): 38–43.

Booth, Adam J., Ryan Hadley, Ashley M. Cornett, Alyssa A. Dreffs, Stephanie A. Matthes, Jessica L. Tsui, Kevin Weiss, et al. (2012) Acellular Normal and Fibrotic Human Lung Matrices as a Culture System for In Vitro Investigation. *American Journal of Respiratory and Critical Care Medicine.* 186(9): 866–76.

Chen, Ku-Chung, Yi-Chu Liao, I-Chung Hsieh, Yung-Song Wang, Ching-Yu Hu, and Suh-Hang Hank Juo. (2012) OxLDL Causes Both Epigenetic Modification and Signaling Regulation on the microRNA-29b Gene: Novel Mechanisms for Cardiovascular Diseases. *Special Section on Post-Translational Modification.* 52(3): 587–95.

Chong, Mark M.W., Guoan Zhang, Sihem Cheloufi, Thomas A. Neubert, Gregory J. Hannon, and Dan R. Littman. (2010) Canonical and Alternate Functions of the microRNA Biogenesis Machinery. *Genes & Development.* 24(17): 1951–60.

Cretu, Alexandra, Paola Castagnino, and Richard Assoian. (2010) Studying the Effects of Matrix Stiffness on Cellular Function Using Acrylamide-Based Hydrogels. *Journal of Visualized Experiments*. 42: 2089.

Davis, Brandi N., Aaron C. Hilyard, Giorgio Lagna, and Akiko Hata. (2008) SMAD Proteins Control DROSHA-Mediated microRNA Maturation. *Nature.* 454(7200): 56–61.

Dupont, Sirio, Leonardo Morsut, Mariaceleste Aragona, Elena Enzo, Stefano Giulitti, Michelangelo Cordenonsi, Francesca Zanconato, et al. (2011) Role of YAP/TAZ in

Mechanotransduction. *Nature*. 474(7350): 179–83.

Fukuda, Toru, Kaoru Yamagata, Sally Fujiyama, Takahiro Matsumoto, Iori Koshida, Kimihiro Yoshimura, Masatomo Mihara, et al. (2007) DEAD-Box RNA Helicase Subunits of the Drosha Complex Are Required for Processing of rRNA and a Subset of microRNAs. *Nat Cell Biol.* 9(5):604–11.

Ha, Minju, and V. Narry Kim. (2014) Regulation of microRNA Biogenesis. *Nat Rev Mol Cell Biol.* 15(8): 509–24.

Heo, Inha, Chirlmin Joo, Jun Cho, Minju Ha, Jinju Han, and V. Narry Kim. (2008) Lin28 Mediates the Terminal Uridylation of Let-7 Precursor MicroRNA. *Molecular Cell.* 32(2):276–84.

Herbert, Kristina M, Genaro Pimienta, Suzanne J DeGregorio, Andrei Alexandrov, and Joan A Steitz. (2013) Phosphorylation of DGCR8 Increases Its Intracellular Stability and Induces a Progrowth miRNA Profile. *Cell Reports.* 5(4): 1070–81.

Horman, Shane R, Maja M Janas, Claudia Litterst, Bingbing Wang, Ian J MacRae, Mary J Sever, David V Morrissey, et al. (2013) Akt-Mediated Phosphorylation of Argonaute 2 down-Regulates Cleavage and up-Regulates Translational Repression of microRNA Targets. *Molecular Cell.* 50(3): 356–67.

Huang, Xiangwei, Naiheng Yang, Vincent F. Fiore, Thomas H. Barker, Yi Sun, Stephan W. Morris, Qiang Ding, Victor J. Thannickal, and Yong Zhou. (2012) Matrix Stiffness–Induced Myofibroblast Differentiation Is Mediated by Intrinsic Mechanotransduction. *American Journal of Respiratory Cell and Molecular Biology.* 47(3): 340–48.

Kalluri, Raghu, and Michael Zeisberg. (2006) Fibroblasts in Cancer. *Nat Rev Cancer* 6(5): 392–401.

Katoh, Takayuki, Yuriko Sakaguchi, Kenjyo Miyauchi, Takeo Suzuki, Shin-ichi Kashiwabara, Tadashi Baba, and Tsutomu Suzuki. (2009) Selective Stabilization of Mammalian microRNAs by 3′ Adenylation Mediated by the Cytoplasmic poly(A) Polymerase GLD-2. *Genes & Development.* 23(4): 433–38.

Liu, Fei, David Lagares, Kyoung Moo Choi, Lauren Stopfer, Aleksandar Marinković, Vladimir Vrbanac, Clemens K. Probst, et al. (2015) Mechanosignaling through YAP and TAZ Drives Fibroblast Activation and Fibrosis. *American Journal of Physiology - Lung Cellular and Molecular Physiology.* 308(4): L344–L357.

Marinković, Aleksandar, Fei Liu, and Daniel J Tschumperlin. (2013) Matrices of Physiologic Stiffness Potently Inactivate Idiopathic Pulmonary Fibrosis Fibroblasts. *American Journal of Respiratory Cell and Molecular Biology.* 48(4): 422–30.

Melo, Sonia A., Catia Moutinho, Santiago Ropero, George A. Calin, Simona Rossi, Riccardo Spizzo, Agustin F. Fernandez, et al. (2010) A Genetic Defect in Exportin-5 Traps Precursor MicroRNAs in the Nucleus of Cancer Cells. *Cancer Cell.* 18(4): 303–15.

Melo, Sonia A, Santiago Ropero, Catia Moutinho, Lauri A Aaltonen, Hiroyuki Yamamoto, George A Calin, Simona Rossi, et al. (2009) A TARBP2 Mutation in Human Cancer Impairs microRNA Processing and DICER1 Function. *Nat Genet.* 41(3): 365–370.

Mori, Masaki, Robinson Triboulet, Morvarid Mohseni, Karin Schlegelmilch, Kriti Shrestha, Fernando D Camargo, and Richard I Gregory. (2014) Hippo Signaling Regulates Microprocessor

and Links Cell Density-Dependent miRNA Biogenesis to Cancer. *Cell.* 156(5): 893–906.

Moroishi, Toshiro, Carsten Gram Hansen, and Kun-Liang Guan. (2015) The Emerging Roles of YAP and TAZ in Cancer. *Nat Rev Cancer.* 15(2): 73–79.

Mott, Justin L, Satoshi Kurita, Sophie Cazanave, Steven F Bronk, Nathan W Werneburg, and Martin E Fernandez-Zapico. (2010) Transcriptional Suppression of Mir-29b-1/mir-29a Promoter by c-Myc, Hedgehog, and NF-kappaB. *Journal of Cellular Biochemistry.* 110(5): 1155–64.

Nho, Richard Seonghun, Mark Peterson, Polla Hergert, and Craig A Henke. (2013) FoxO3a (Forkhead Box O3a) Deficiency Protects Idiopathic Pulmonary Fibrosis (IPF) Fibroblasts from Type I Polymerized Collagen Matrix-Induced Apoptosis via Caveolin-1 (cav-1) and Fas. *PLoS ONE.* 8(4): e61017.

Oak, Sameer R, Lynne Murray, Athula Herath, Matthew Sleeman, Ian Anderson, Amrita D Joshi, Ana Lucia Coelho, et al. (2011) A Micro RNA Processing Defect in Rapidly Progressing Idiopathic Pulmonary Fibrosis. *PLoS ONE.* 6(6): e21253.

Pandit, Kusum V., and Jadranka Milosevic. (2015) MicroRNA Regulatory Networks in Idiopathic Pulmonary Fibrosis. *Biochemistry and Cell Biology.* 93(2): 129–37.

Parker, Matthew W., Daniel Rossi, Mark Peterson, Karen Smith, Kristina Sikström, Eric S. White, John E. Connett, Craig A. Henke, Ola Larsson, and Peter B. Bitterman. (2014) Fibrotic Extracellular Matrix Activates a Profibrotic Positive Feedback Loop. *The Journal of Clinical Investigation.* 124(4): 1622–1635.

Paroo, Zain, Xuecheng Ye, She Chen, and Qinghua Liu. (2009) Phosphorylation of the Human

microRNA-Generating Complex Mediates MAPK/Erk Signaling. *Cell.* 139(1): 112–122.

Qi, Hank H, Pat P Ongusaha, Johanna Myllyharju, Dongmei Cheng, Outi Pakkanen, Yujiang Shi, Sam W Lee, Junmin Peng, and Yang Shi. (2008) Prolyl 4-Hydroxylation Regulates Argonaute 2 Stability. *Nature.* 455(7211): 421–424.

Rosas, Ivan O., Robert M. Kottman, and Patricia J. Sime. (2013) New Light Is Shed on the Enigmatic Origin of the Lung Myofibroblast. *American Journal of Respiratory and Critical Care Medicine.* 188(7): 765–766.

Schaffer, Justin M., Steve K. Singh, Bruce A. Reitz, Roham T. Zamanian, and Hari R. Mallidi. (2015) Single- vs Double-Lung Transplantation in Patients With Chronic Obstructive Pulmonary Disease and Idiopathic Pulmonary Fibrosis Since the Implementation of Lung Allocation Based on Medical Need. *The Journal of the American Medical Association.* 313: 936–48.

Tang, Xiaoli, Ming Li, Lynne Tucker, and Bharat Ramratnam. (2011) Glycogen Synthase Kinase 3 Beta (GSK3β) Phosphorylates the RNAase III Enzyme Drosha at S300 and S302. *PLoS ONE.* 6(6): e20391.

Tang, Xiaoli, Sicheng Wen, Dong Zheng, Lynne Tucker, Lulu Cao, Dennis Pantazatos, Steven F Moss, and Bharat Ramratnam. (2013) Acetylation of Drosha on the N-Terminus Inhibits Its Degradation by Ubiquitination. *PLoS ONE.* 8(8): e72503.

Tang, Xiaoli, Yingjie Zhang, Lynne Tucker, and Bharat Ramratnam. (2010) Phosphorylation of the RNase III Enzyme Drosha at Serine300 or Serine302 Is Required for Its Nuclear Localization. *Nucleic Acids Research*. 38(19): 6610–6619.

Tumaneng, Karen, Karin Schlegelmilch, Ryan C. Russell, Dean Yimlamai, Harihar Basnet, Navin Mahadevan, Julien Fitamant, Nabeel Bardeesy, Fernando D. Camargo, and Kun-Liang Guan. (2012) YAP Mediates Crosstalk between the Hippo and PI(3)K–TOR Pathways by Suppressing PTEN via miR-29. *Nat Cell Biol.* 14(12): 1322–1329.

Tzouvelekis, Argyris, Francesco Bonella, and Paolo Spagnolo. (2015) Update on Therapeutic Management of Idiopathic Pulmonary Fibrosis. *Therapeutics and Clinical Risk Management.* 11: 359–370.

Van Kouwenhove, Marieke, Martijn Kedde, and Reuven Agami. (2011) MicroRNA Regulation by RNA-Binding Proteins and Its Implications for Cancer. *Nat Rev Cancer.* 11(9):644–56.

Wada, Taeko, Jiro Kikuchi, and Yusuke Furukawa. (2012) Histone Deacetylase 1 Enhances microRNA Processing via Deacetylation of DGCR8. *EMBO Reports.* 13(2): 142–149.

Wang, Yangming, Rostislav Medvid, Collin Melton, Rudolf Jaenisch, and Robert Blelloch. (2007) DGCR8 Is Essential for microRNA Biogenesis and Silencing of Embryonic Stem Cell Self-Renewal. *Nature Genetics.* 39(3): 380–385.

Wolters, Paul J, Harold R Collard, and Kirk D Jones. (2014) Pathogenesis of Idiopathic Pulmonary Fibrosis. *Annual Review of Pathology.* 9: 157–179.

Xia, Hong, Vidya Bodempudi, Alexey Benyumov, Polla Hergert, Damien Tank, Jeremy Herrera, Jeff Braziunas, et al. (2014) Identification of a Cell-of-Origin for Fibroblasts Comprising the Fibrotic Reticulum in Idiopathic Pulmonary Fibrosis. *The American Journal of Pathology.* 184(5): 1369–83.

Xia, Hong, Deanna Diebold, Richard Nho, David Perlman, Jill Kleidon, Judy Kahm, Svetlana Avdulov, et al. (2008) Pathological Integrin Signaling Enhances Proliferation of Primary Lung Fibroblasts from Patients with Idiopathic Pulmonary Fibrosis. *The Journal of Experimental Medicine.* 205(7): 1659–1672.

Xiao, Jun, Xiao-Ming Meng, Xiao R Huang, Arthur CK Chung, Yu-Lin Feng, David SC Hui, Cheuk-Man Yu, Joseph JY Sung, and Hui Y Lan. (2012) miR-29 Inhibits Bleomycin-Induced Pulmonary Fibrosis in Mice. *Molecular Therapy.* 20(6): 1251–1260.

Zhao, Bin, Li Li, Karen Tumaneng, Cun-Yu Wang, and Kun-Liang Guan. (2010) A Coordinated Phosphorylation by Lats and CK1 Regulates YAP Stability through SCF(β-TRCP). *Genes & Development.* 24(1): 72–85.